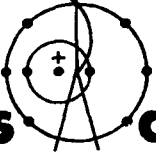


LA-4726 (ENDF-175)

**C. 3**

CIC-14 REPORT COLLECTION  
**REPRODUCTION  
COPY**

A Preliminary Evaluation of the Neutron  
and Photon-Production Cross Sections  
for Aluminum



**los alamos**  
**scientific laboratory**  
of the University of California  
LOS ALAMOS, NEW MEXICO 87544

UNITED STATES  
ATOMIC ENERGY COMMISSION  
CONTRACT W-7405-ENG. 36

This report was prepared as an account of work sponsored by the United States Government. Neither the United States nor the United States Atomic Energy Commission, nor any of their employees, nor any of their contractors, subcontractors, or their employees, makes any warranty, express or implied, or assumes any legal liability or responsibility for the accuracy, completeness or usefulness of any information, apparatus, product or process disclosed, or represents that its use would not infringe privately owned rights.

Printed in the United States of America. Available from  
National Technical Information Service  
U. S. Department of Commerce  
5285 Port Royal Road  
Springfield, Virginia 22151  
Price: Printed Copy \$3.00; Microfiche \$0.95

LA-4726 (ENDF-175)

UC-34

ISSUED: December 1972



# A Preliminary Evaluation of the Neutron and Photon-Production Cross Sections for Aluminum



by

P. G. Young  
D. G. Foster, Jr.



This work was supported by the Defense Nuclear Agency under Subtask PC102.

## CONTENTS

ABSTRACT	1
1. INTRODUCTION	1
2. NEUTRON CROSS SECTIONS	1
2.1. Total Cross Section	1
2.2. Elastic Scattering Cross Section	5
2.3. Radiative-Capture Cross Section	8
2.4. Inelastic Scattering Cross Sections	13
2.4.1. The $^{27}\text{Al}(n,n')$ Cross Sections for $E_x(^{27}\text{Al}) < 5$ MeV	13
2.4.2. The $^{27}\text{Al}(n,n')$ Cross Sections for $E_x(^{27}\text{Al}) > 5$ MeV	14
2.5. The $^{27}\text{Al}(n,np)^{26}\text{Mg}$ , $^{27}\text{Al}(n,\alpha)^{23}\text{Na}$ , and $^{27}\text{Al}(n,2n)^{26}\text{Al}$ Cross Sections	15
2.6. The $^{27}\text{Al}(n,p)^{27}\text{Mg}$ Cross Section	18
2.7. The $^{27}\text{Al}(n,d)^{26}\text{Mg}$ and $^{27}\text{Al}(n,t)^{25}\text{Mg}$ Cross Sections	18
2.8. The $^{27}\text{Al}(n,\alpha)^{24}\text{Na}$ Cross Section	20
3. PHOTON-PRODUCTION CROSS SECTIONS AND ENERGY SPECTRA	21
3.1. Photon Production from the $^{27}\text{Al}(n,\gamma)^{28}\text{Al}$ Reaction	21
3.2. Photon Production from $^{27}\text{Al}(n,x\gamma)$ Reactions	22
3.2.1. Discrete Photons from $^{27}\text{Al}(n,x\gamma)$ Reactions	22
3.2.2. Continuum Photons from $^{27}\text{Al}(n,x\gamma)$ Reactions	29
4. NEUTRON ENERGY DISTRIBUTIONS	29
5. ANGULAR DISTRIBUTIONS	30
5.1. Elastic Neutron Angular Distributions	31
5.2. Nonelastic Neutron Angular Distributions	31
5.3. Secondary Photon Angular Distributions	32
6. DISCUSSION	33
ACKNOWLEDGMENTS	34
REFERENCES	34

A PRELIMINARY EVALUATION OF THE  
NEUTRON AND PHOTON-PRODUCTION CROSS SECTIONS  
FOR ALUMINUM

by

P. G. Young and D. G. Foster, Jr.

ABSTRACT

A preliminary evaluation of the neutron-induced cross sections of  $^{27}\text{Al}$  has been completed for the energy range  $10^{-5}$  eV to 20 MeV. The evaluation includes specification of energy and angular distributions for secondary neutrons and photons. The recommended data are based mainly on experiment, and extensive comparisons with measured results are provided. In certain areas model calculations were used to augment the experimental data. The evaluated results are available on magnetic tape in ENDF/B(III) format.

## 1. INTRODUCTION

A preliminary evaluation of the neutron-induced cross sections for  $^{27}\text{Al}$  has been completed for the energy region from  $10^{-5}$  eV to 20 MeV. The evaluation includes specification of angular and energy distributions for secondary gamma rays, as well as for secondary neutrons. The data are in ENDF/B format and have been filed with the National Neutron Cross Section Center at Brookhaven (MAT 1135) and with the Defense Nuclear Agency's (DNA) military applications library at the Radiation Shielding Information Center in Oak Ridge (MAT 4135).

The purpose of this work was to provide DNA with a preliminary aluminum evaluation that contains consistent neutron and photon-production data and that includes consideration of several important new measurements. Because time was limited, we did not perform a complete literature survey, and in some areas previous evaluations were accepted without improvement. The treatment in the resolved-resonance region is sketchy with some fine structure smoothed out, and only a bare minimum of supporting nuclear-model calculations were carried out. Therefore, the evaluation should be regarded as tentative.

A summary of the Q-values and thresholds for the significant neutron reactions with aluminum is given

in Table I. Because natural aluminum is 100%  $^{27}\text{Al}$ , only reactions with  $^{27}\text{Al}$  are listed. The reactions listed in Table I, together with the total cross section, were evaluated in varying amounts of detail. The evaluated results are based mainly on experimental data although simple model calculations were used in some areas to supplement the measurements. Several charged-particle processes with thresholds above 14 MeV, such as the  $(n, ^3\text{He})$ ,  $(n, 2p)$ ,  $(n, 2\alpha)$ , and  $(n, p\alpha)$  reactions, are omitted from Table I. These reactions are expected to have small cross sections and are not treated explicitly in the evaluation. The detailed considerations that went into the evaluation are described in the following sections.

## 2. NEUTRON CROSS SECTIONS

### 2.1. Total Cross Section

Below 0.5 MeV, the total cross section is based mainly on the work of Merrison and Wiblin (Me52) from 1.1 eV to 3.6 keV, and of Hibdon (Hi59, Hi64) between 1.5 and 450 keV, which we normalized to each other over their small overlap region. To tie these to our evaluation in the MeV region, we used the results of Chien and Smith (Ch66) to bridge a gap between 450 and 460 keV. However, to produce general agreement, we had to lower their results by 5.3% and

TABLE I  
Q-VALUES AND THRESHOLDS OF IMPORTANT  
NEUTRON-INDUCED REACTIONS FOR  $^{27}\text{Al}$

Reaction	Q-Value (MeV)	Threshold (MeV)
$^{27}\text{Al}(n,\gamma)^{28}\text{Al}$	7.724	---
$^{27}\text{Al}(n,n)^{27}\text{Al}$	0.	---
$^{27}\text{Al}(n,n')^{27}\text{Al}^*$	-0.843	0.875
$^{27}\text{Al}(n,p)^{27}\text{Mg}$	-1.831	1.899
$^{27}\text{Al}(n,d)^{26}\text{Mg}$	-6.046	6.272
$^{27}\text{Al}(n,t)^{25}\text{Mg}$	-10.884	11.291
$^{27}\text{Al}(n,\alpha)^{24}\text{Na}$	-3.131	3.248
$^{27}\text{Al}(n,2n)^{26}\text{Al}$	-13.057	13.545
$^{27}\text{Al}(n,np)^{26}\text{Mg}$	-8.271	8.580
$^{27}\text{Al}(n,n\alpha)^{23}\text{Na}$	-10.101	10.479

raise those of Merrison and Wiblin by 11.3%. The work of Hibdon and Muehlhause (H149) and Rayburn and Wollan (Ra65) indicate that below 100 keV this composite may be about 5% too high. Unfortunately, the

absolute cross sections from the time-of-flight work of Garg et al. (Ga65) are untrustworthy within roughly 20%; therefore we cannot use them to resolve this problem. Instead, we have used the Garg data mainly to supply the fine structure details below 150 keV. We have not corrected Hibdon's energy scale (H159, H164) above 100 keV, although the scale of Garg et al. (Ga65) is almost certainly more accurate.

From our total cross section above 1 eV, we deduced a potential-scattering cross section of 1.511 b. By combining this value with the 2200-m/sec radiative-capture cross section of 232 mb from the evaluation by Goldman et al. (Go71; see Sec. 2.3), and assuming  $1/v$  variation for the latter up to about 10 eV, we synthesized the total cross section between  $10^{-5}$  eV and 1 eV. This region inherits the 5% uncertainty of the total cross section that is present in the keV region.

Figure 1 shows the resulting evaluated curve below 1 keV, together with the previous ENDF/B(II)

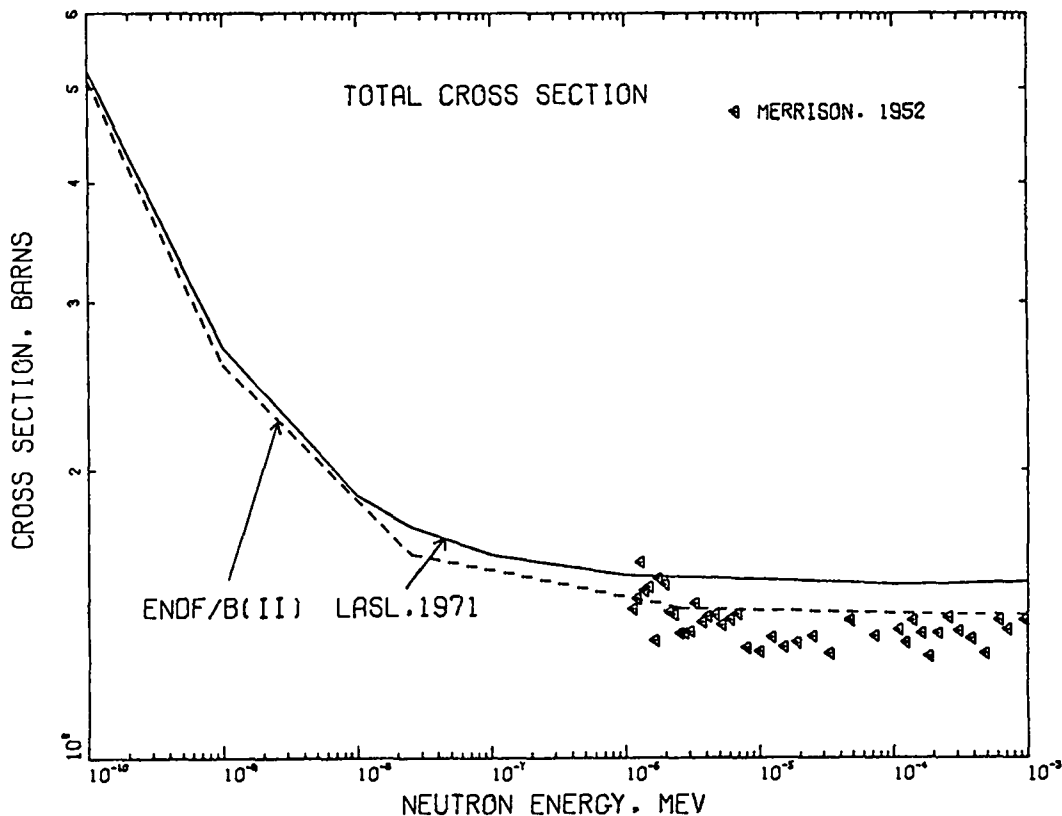


Fig. 1. Measured and evaluated total cross section for  $^{27}\text{Al}$  from  $10^{-4}$  eV to 1 keV. The experimental data are averages of two adjacent points.

evaluation and the data of Merrison and Wiblin (Me52). The differences result primarily from the chain of normalizations that we applied to the older data to force agreement with more recent data in the MeV range. In this and in all subsequent figures, the measurements are displayed in their original (unnormalized) form.

The measured and evaluated total cross sections from 1 to 100 keV are shown in Fig. 2. The data of Garg et al. (Ga65) are impossible to plot individually on this scale, so we have given many-point averages that fail to justify the fine structure shown in the evaluated curves, although the data of

Garg et al. form the basis of the curves. The ENDF/B (II) curve follows the Garg data without correction for their "tilt" relative to the other measurements. This anomaly might have been caused by uncorrected dead-time errors in the Columbia University (Ga65) work.

The evaluated total cross section in the MeV region is based on a composite of three recent measurements that agree to within  $\pm 1\%$  in their regions of mutual overlap. The results of Schwartz (Sc70) and Foster and Glasgow (Fo71) were obtained by time-of-flight techniques using continuous spectra of incident neutrons. We discarded the erratic portion of Schwartz's data above 10 MeV, where background

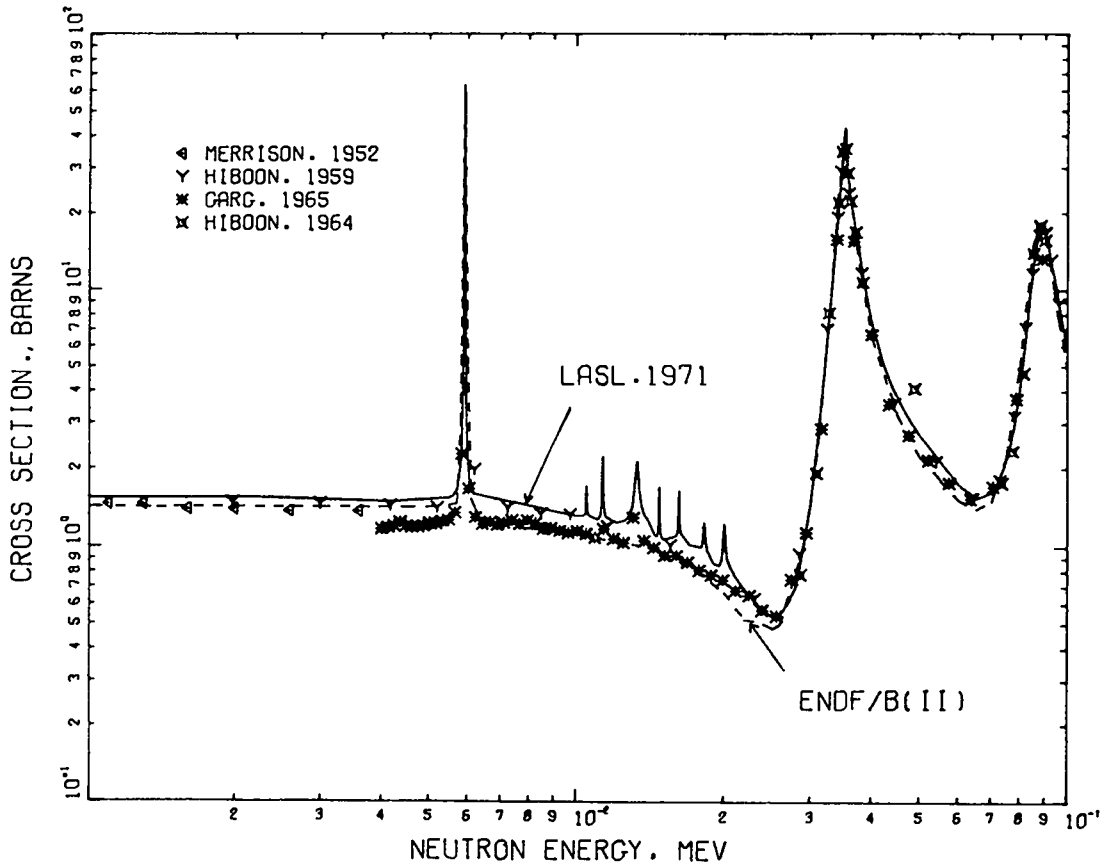


Fig. 2. Measured and evaluated total cross section for  $^{27}\text{Al}$  from 1 to 100 keV. The experimental data are averages of 30 adjacent points for the Garg (Ga65) results, 5 points for the Hibdon (Hi59) results, and 4 points for the Hibdon (Hi64) results.

was a severe problem in that measurement. The third experiment used in the composite is that of Carlson and Barschall (Ca67), which is one of the few extensive measurements made point-by-point with monoenergetic neutrons that agrees systematically with modern time-of-flight data. A fourth data set, the detailed results from Karlsruhe by Cierjacks et al. (Ci68), was found, even after the latest round of dead-time corrections, still to lie systematically higher than our composite standard by amounts varying between 1.5 and 4%. To preserve the best available resolution, however, we normalized the Cierjacks data piecewise to our composite and used the results between 0.46 and 7.5 MeV for our final evaluation. Above 7.5 MeV, the energy resolution of the Carlson and Barschall measurement is as good as that of the Karlsruhe measurement, so we used a composite of their normalized data up to 14 MeV, and the normal-

ized Karlsruhe values alone from 14 to 20 MeV. We estimate the overall accuracy between 0.5 and 20 MeV to be about 1%.

Figure 3 gives the measured and evaluated total cross section from 0.05 to 0.50 MeV. As noted earlier, we have not corrected Hibdon's energy scale (Hi59, Hi64), although we followed his data because their resolution is better than Garg's in this region. The extensive measurements of Cierjacks et al. (Ci68) and Schwartz (Sc70) begin at the right edge of Fig. 3.

The synthetic total cross section below the first resonance at 5.9 keV is already smooth. In the resolved-resonance region, we smoothed the data by using approximate single-level fits to the peaks, joined together by sliding-polynomial fits between resonances. Above the resolved-resonance region, sliding-polynomial smoothing was used. We tried to

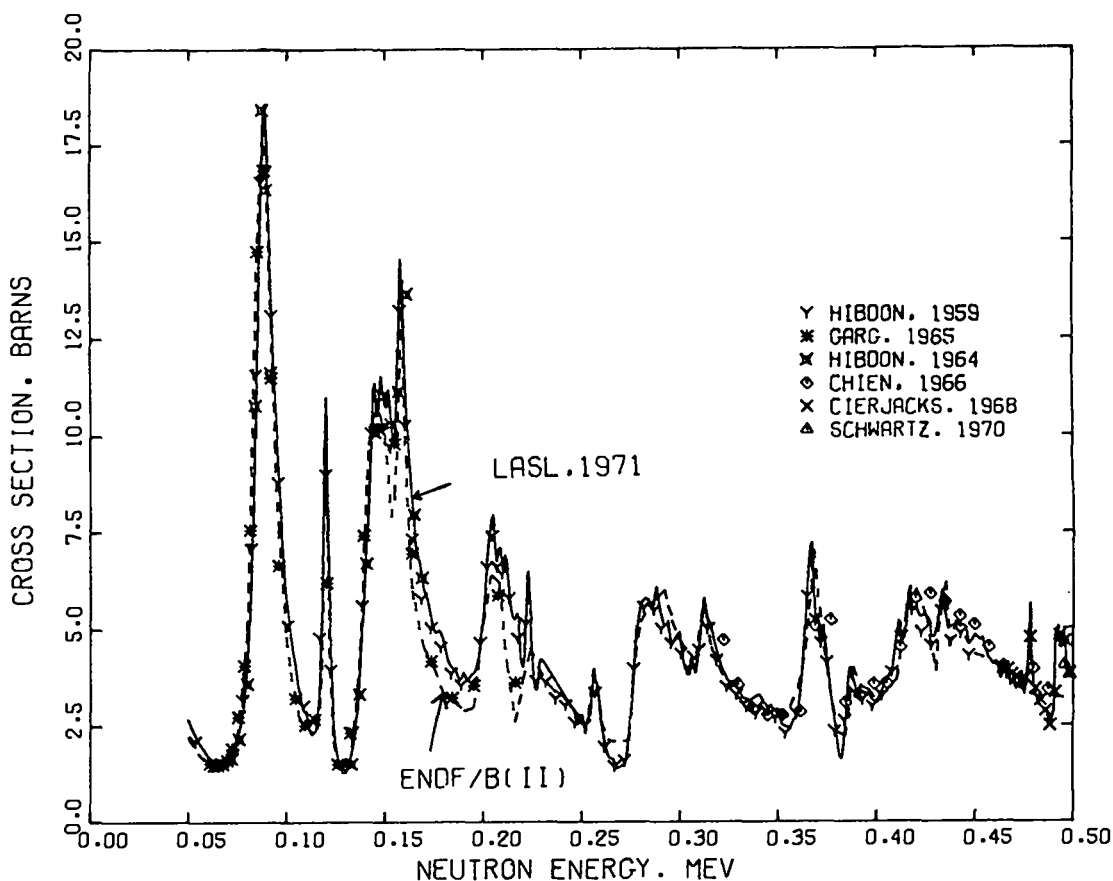


Fig. 3. Measured and evaluated total cross section for  $^{27}\text{Al}$  from 0.05 to 0.50 MeV. The experimental data are averages of 5 points for the Hibdon (Hi59) results, 10 points for Garg (Ga65), 4 points for Hibdon (Hi64), 5 points for Chien (Ch66), 15 points for Cierjacks (Ci68), and 10 points for Schwartz (Sc70).

preserve the fluctuations between 0.5 and 3 MeV but they are represented on such a coarse mesh that linear interpolation may give errors of as much as 2%. Above 3 MeV, we drastically oversmoothed the fluctuations to reduce the number of points in the evaluated file.

The transition region from resolved resonances to fluctuations, covering the energy region from 0.5 to 4 MeV, is shown in Figs. 4-6. Throughout this range our evaluation follows the Karlsruhe data (Ci68) normalized to Schwartz's results (Sc70). Figure 6 includes the beginning of the moderate-resolution results of Foster and Glasgow (Fo71) and illustrates the good average agreement of the Foster and Schwartz time-of-flight measurements. It also illustrates the oversmoothing of fluctuations\* above 3 MeV, which can still be seen in the multi-point averages of the Karlsruhe data.

Figure 7 covers the energy range from 4 to 9 MeV. The measurement of Carlson and Barschall (Ca67),

\* Figures 4-8 have suppressed zero points on the cross-section scales, which overemphasizes the fluctuations.

which is the third constituent of our composite "standard," begins near 4.5 MeV and closely follows the fluctuations in the data of Cierjacks et al. (Ci68).

The total cross section for the remaining energy range from 9 to 20 MeV is given in Fig. 8. The disagreement between our evaluation and the ENDF/B(II) data set that began near 7.5 MeV is even more apparent in Fig. 8. The results of Carlson and Barschall (Ca67) and Foster and Glasgow (Fo71) continue to display good agreement, whereas Schwartz's data (Sc70) become increasingly discordant, reflecting the background problem mentioned earlier. The ENDF/B(II) curve follows older measurements, not shown here, and reflects the relative ease of making accurate monoenergetic measurements near 14 MeV as compared to the comparatively inaccessible region near 10 MeV.

### 2.2. The Elastic Scattering Cross Section

The potential scattering cross section in the eV energy region was determined to be 1.511 b from the analysis described in Sec. 2.1. At other energies below 5 MeV, the evaluated elastic cross section

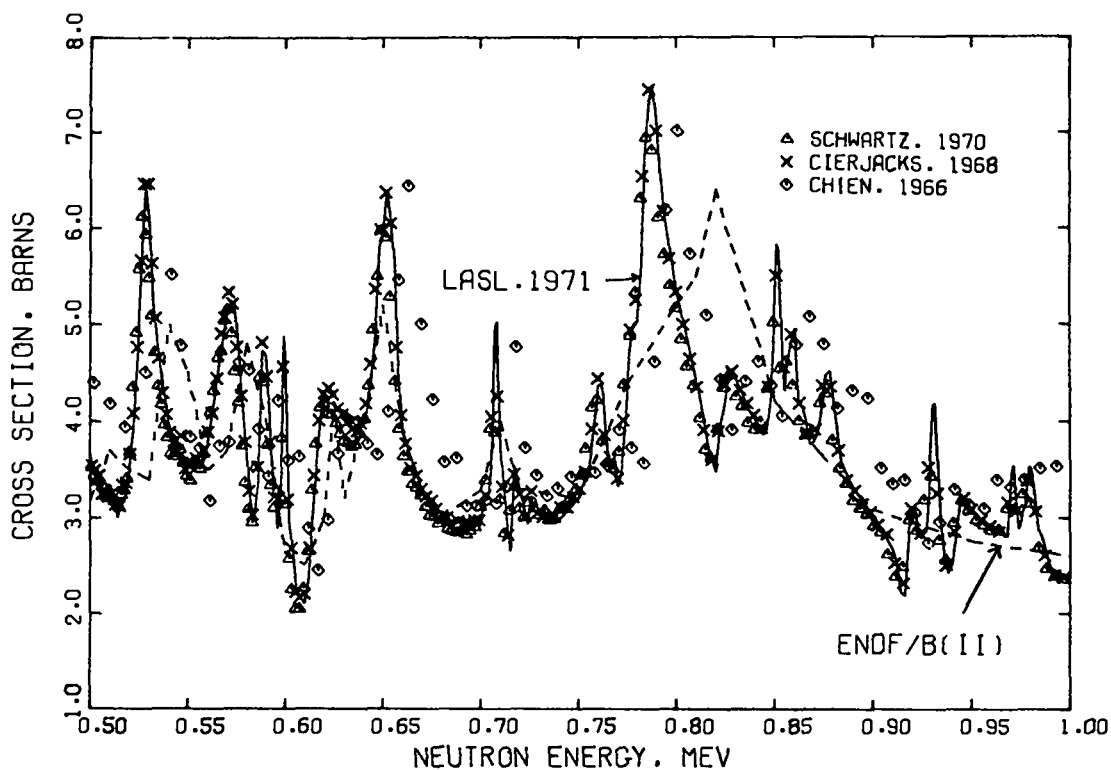


Fig. 4. Measured and evaluated total cross section for  $^{27}\text{Al}$  from 0.5 to 1.0 MeV. The experimental data are averages of 6 points for the Schwartz (Sc70) results, 10 points for Cierjacks (Ci68), and 5 points for Chien (Ch66).

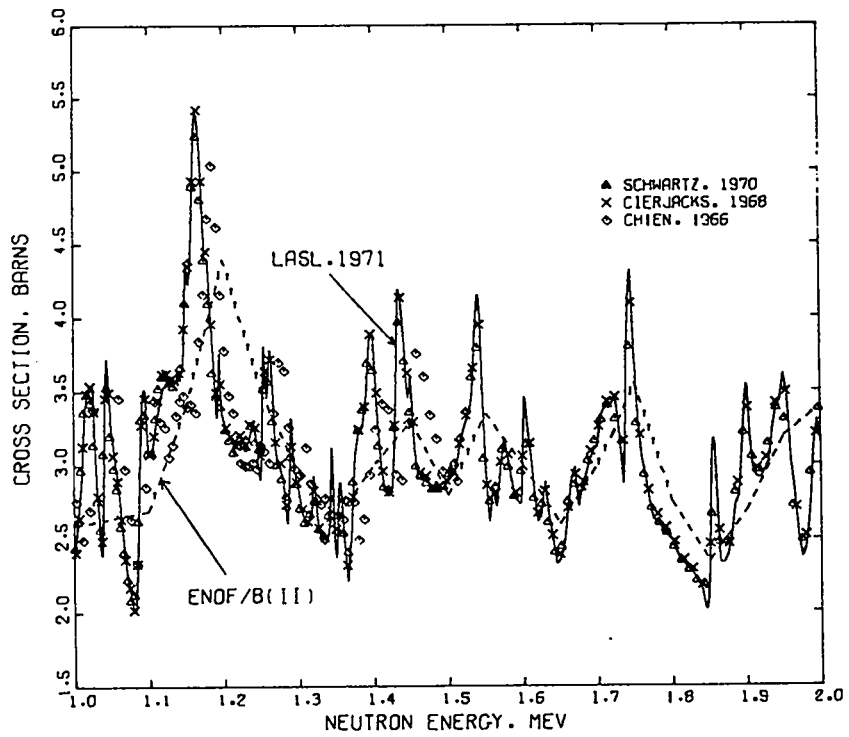


Fig. 5. Measured and evaluated total cross section for  $^{27}\text{Al}$  from 1 to 2 MeV. The experimental data are averages of 6 points for the Schwartz (Sc70) results, 10 points for Cierjacks (C168), and 5 points for Chien (Ch66).

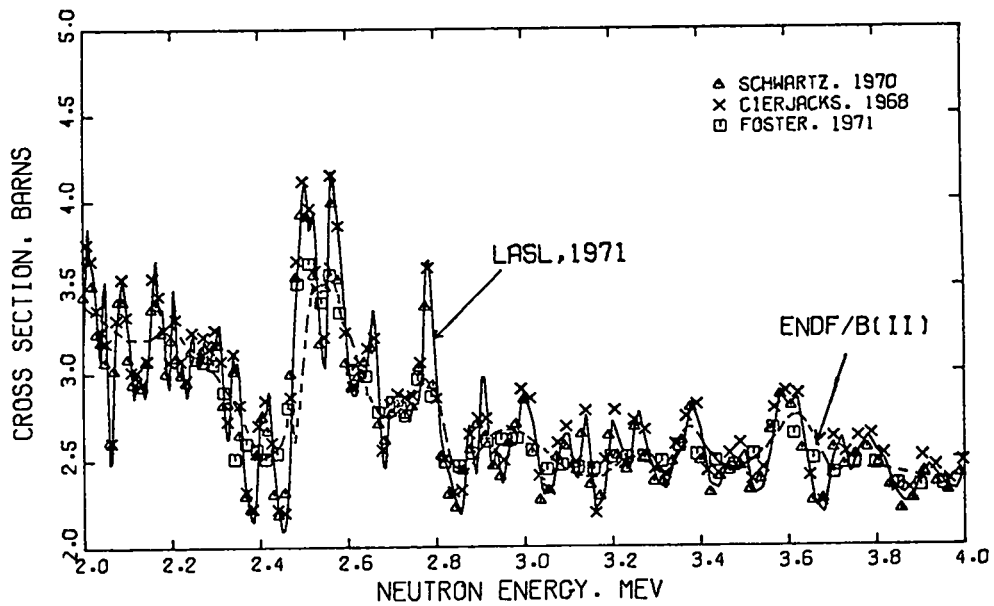


Fig. 6. Measured and evaluated total cross section for  $^{27}\text{Al}$  from 2 to 4 MeV. The experimental data are averages of 5 points for the Schwartz (Sc70) results, 8 points for Cierjacks (C168), and 2 points for Foster (Fo71).

was determined by subtracting the sum of the individual reaction cross sections from the evaluated total cross section. Discussion of the evaluation of the individual reaction channels is given in Secs. 2.3 through 2.8.

The evaluated elastic cross section from 50 keV to 5 MeV is compared in Figs. 9-12 to the ENDF/B(II) evaluation and to the available measurements. The experimental points for the elastic cross section in these and in subsequent figures were obtained by integrating angular-distribution measurements. The agreement between the elastic measurements and the evaluated curve is good in this region, although the resolution of the measurements is generally too poor to verify the detailed structure in the cross section. The structure is taken, of course, from the high-resolution total-cross-section measurements.

The evaluated nonelastic cross section below 5 MeV is compared to experimental data in Fig. 13.

The curve was obtained by summing the partial reaction cross sections and was used to determine the elastic, as described above. Except for Pasechnik's (Pa55) measurement at 2.5 MeV, the agreement between the evaluated curve and the nonelastic measurements is reasonably good. Detailed information on the fine structure in the nonelastic cross section is not available, and unknown structure might account for the inconsistencies in Fig. 13.

From 5 to 20 MeV, the evaluated elastic cross section was determined from elastic and nonelastic measurements, assuming the total cross section to be a known quantity. From 5 to 9 MeV, additional nonelastic information was included in the analysis by combining the evaluated (n,p) and (n, $\alpha$ ) cross sections with the total (n,n') cross section, as estimated by Dickens (Di71) from the sum of all ground-state transitions in (n,n' $\gamma$ ) measurements (see Sec. 2.4). The resulting elastic cross section from 5 to

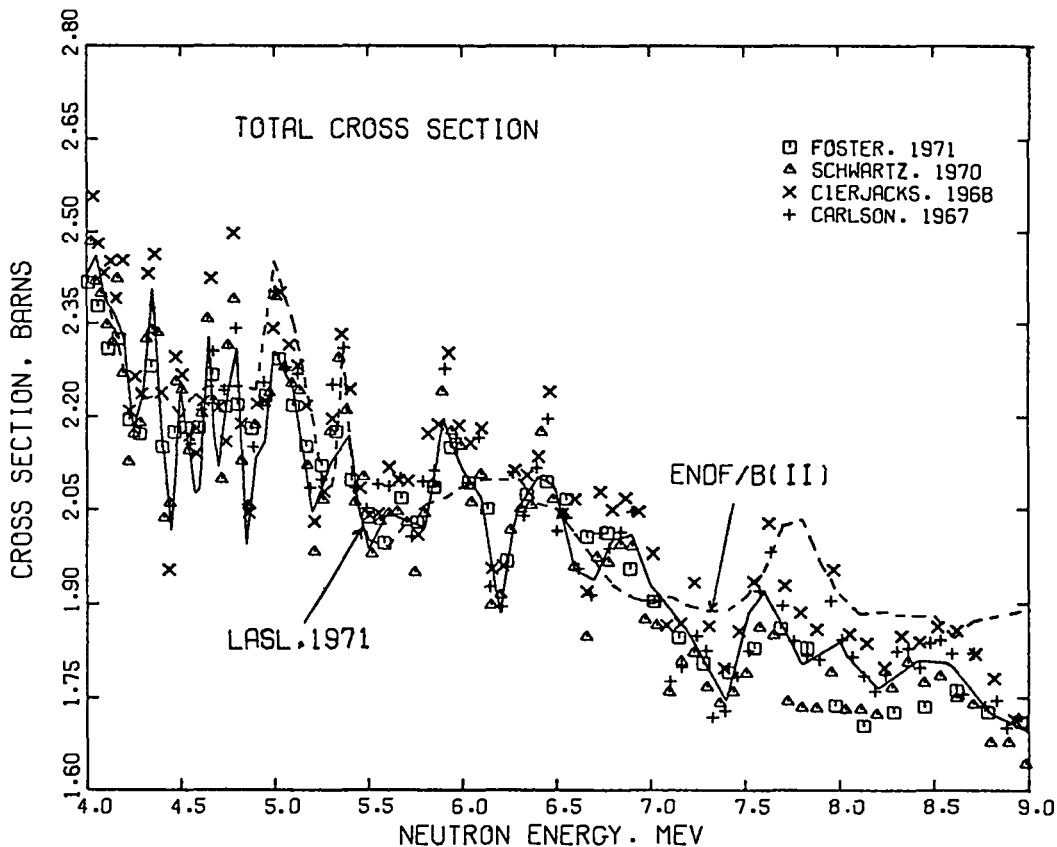


Fig. 7. Measured and evaluated total cross section for  $^{27}\text{Al}$  from 4 to 9 MeV. The experimental data are averages of 2 points for the Foster (Fo71) results, 5 points for Schwartz (Sc70), 8 points for Cierjacks (Ci68), and 3 points for Carlson (Ca67).

20 MeV is compared to the measurements in Fig. 14, and the nonelastic cross section for the same energy region is given in Fig. 15. The evaluated elastic that results from this analysis is somewhat lower than is usual, falling below half the total cross section at neutron energies above 8 MeV. Therefore, we prejudiced the evaluation slightly toward higher values at some energies. Even lower values for the elastic are suggested, however, by the Nellis (Ne71) measurements at 9 and 11 MeV, and the recent result of Glasgow et al. (G172) at 9 MeV, which was not available for the evaluation, supports our choice. We extrapolated the elastic curve to 20 MeV by joining the lower-energy results smoothly to a value of  $\sigma_{\text{tot}}/2$  at 20 MeV. The evaluated elastic curve in Fig. 14 differs significantly from ENDF/B(II) at some energies.

### 2.3. Radiative-Capture Cross Section

In Sec. 2.1, we adopted the 232-mb 2200-m/sec capture cross section from an unpublished evaluation by Goldman et al. (Go71) and assigned to it a  $1/v$  variation, as shown in Fig. 16. The  $1/v$  decrease

continues to about 0.1 keV, where it meets the wings of the 5.9-keV resonance shown in Fig. 17. From 4 to 140 keV, we used the data of Block (B168) for the integrated cross section, taking the widths and actual energies of the resonances from the total-cross-section measurements of Garg et al. (Ga65). Thus, the first resonance comes at 5.906 keV with a peak capture cross section of 1480 mb, rather than the 380 mb found with Block's resolution. As shown in Figs. 17 and 18, the result in the low keV region is not drastically different from the ENDF/B(II) evaluation. Most of the difference comes from improved resolution and more accurate energies.

Figure 19 shows the region from 0.1 to 1 MeV. Here we relied mainly on Henkel's work (He50, He53). Because the cross section is only a few millibarns or less, we did not attempt to follow the fine structure, as did the older ENDF/B evaluation, but instead have averaged rather severely. In Fig. 20, we relied on the measurement of Calvi et al. (Ca62) for the cross section from 3.5- to 5-MeV, and then arbitrarily assumed a linear rise through the cluster of

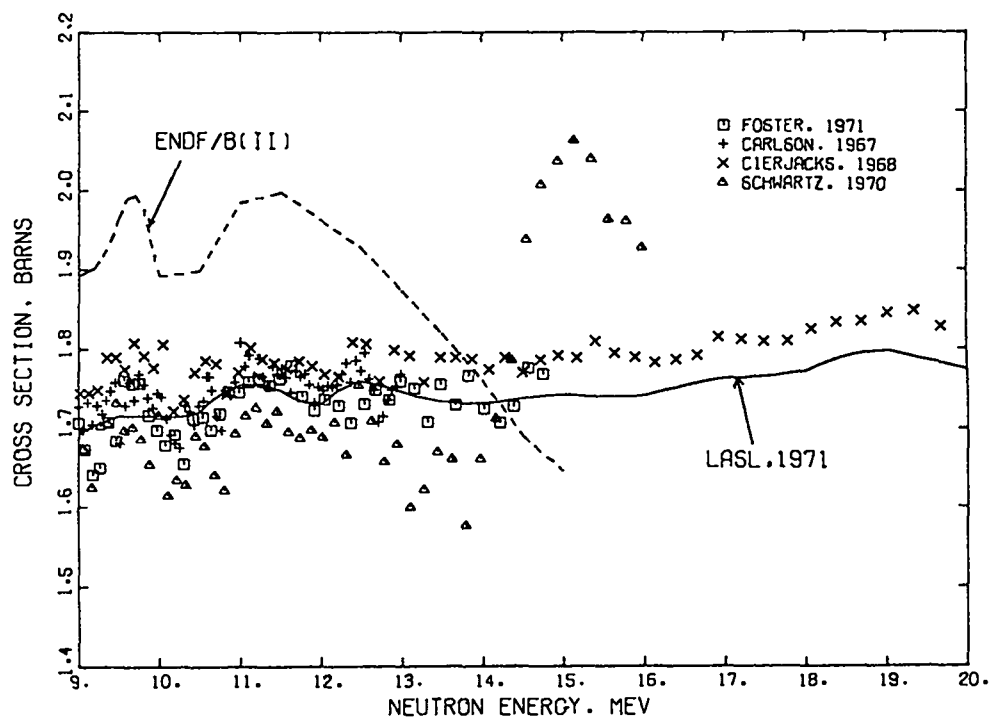


Fig. 8. Measured and evaluated total cross section for  $^{27}\text{Al}$  from 9 to 20 MeV. The experimental data are averages of 3 points for the Carlson (Ca67) results, 8 points for Cierjacks (C168), and 5 points for Schwartz (Sc70).

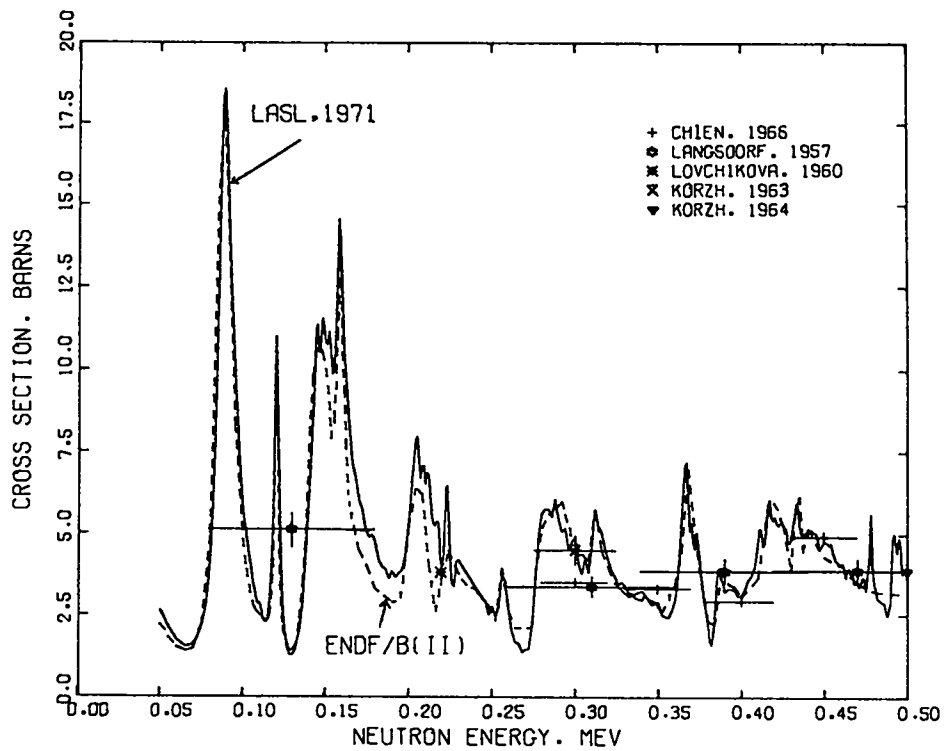


Fig. 9. Measured and evaluated elastic scattering cross section for  $^{27}\text{Al}$  from 0.05 to 0.50 MeV.

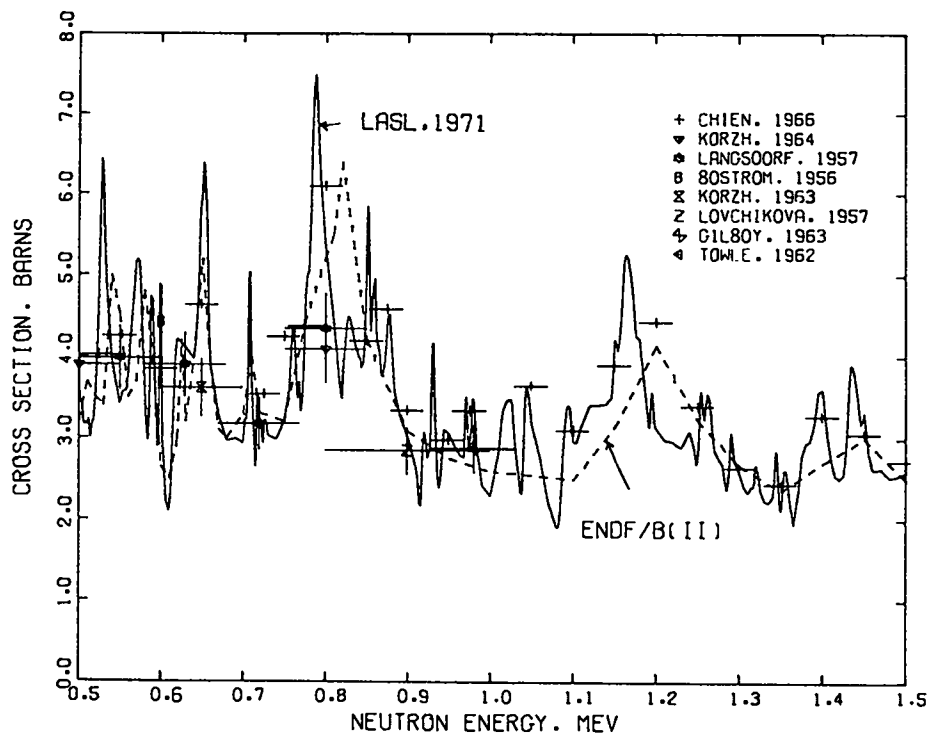


Fig. 10. Measured and evaluated elastic scattering cross section for  $^{27}\text{Al}$  from 0.5 to 1.5 MeV.

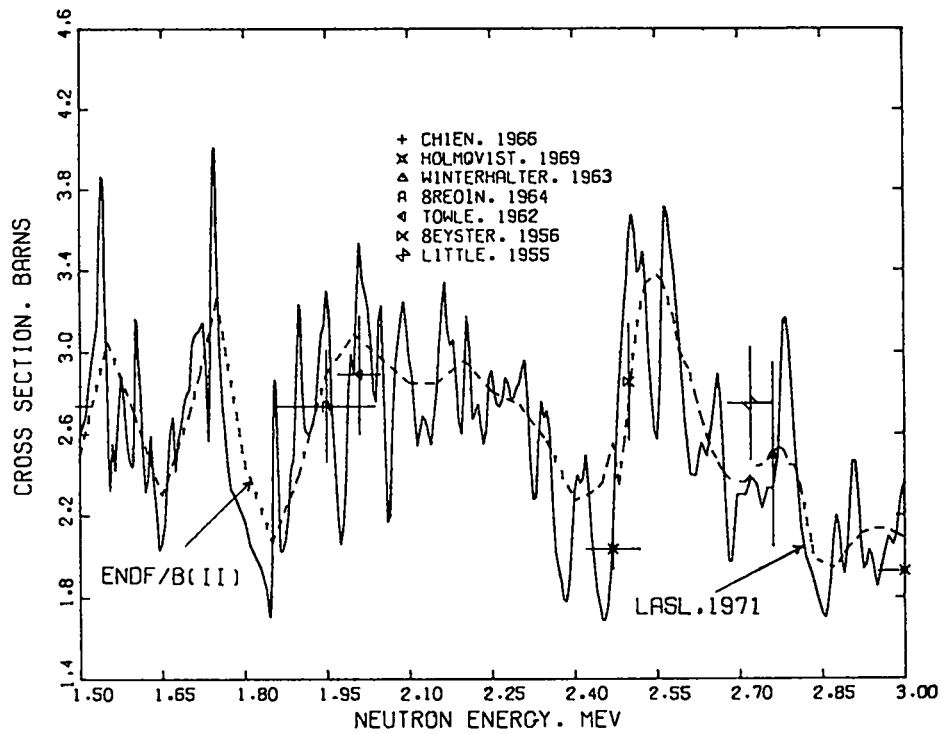


Fig. 11. Measured and evaluated elastic scattering cross section for  $^{27}\text{Al}$  from 1.5 to 3.0 MeV.

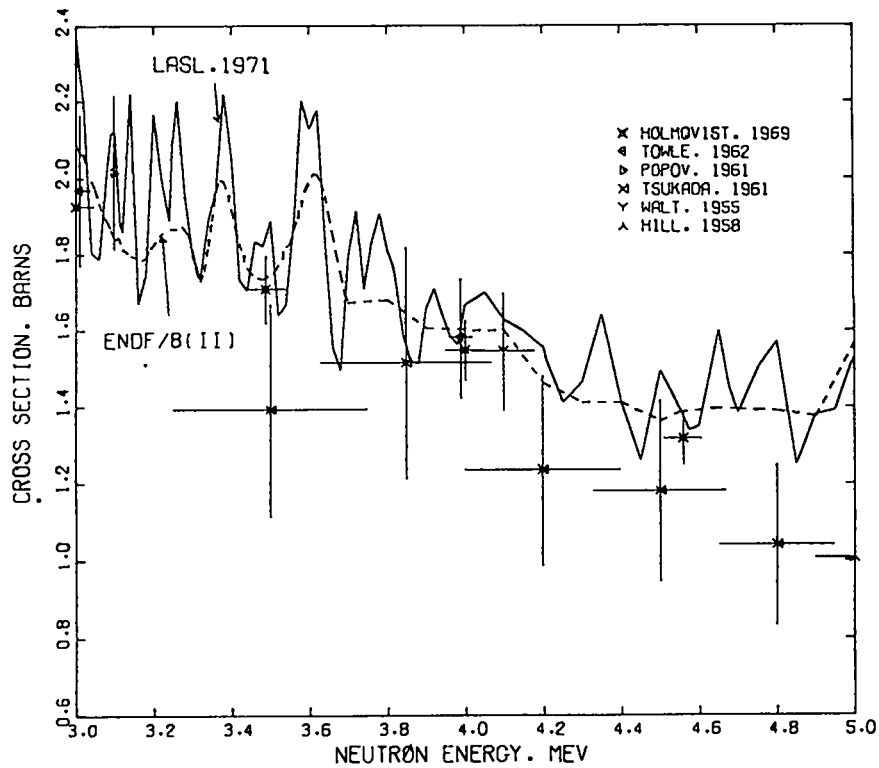


Fig. 12. Measured and evaluated elastic scattering cross section for  $^{27}\text{Al}$  from 3 to 5 MeV.

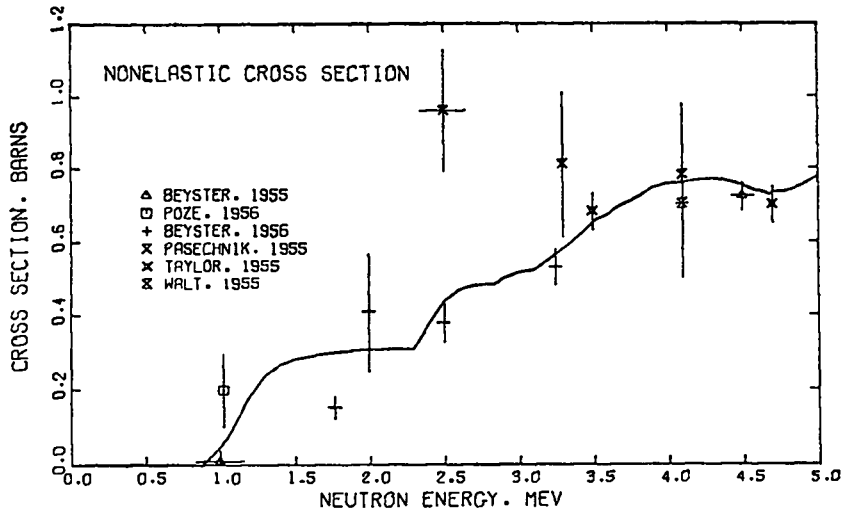


Fig. 13. Measured and evaluated nonelastic cross section for  $^{27}\text{Al}$  from 0.5 to 5.0 MeV.

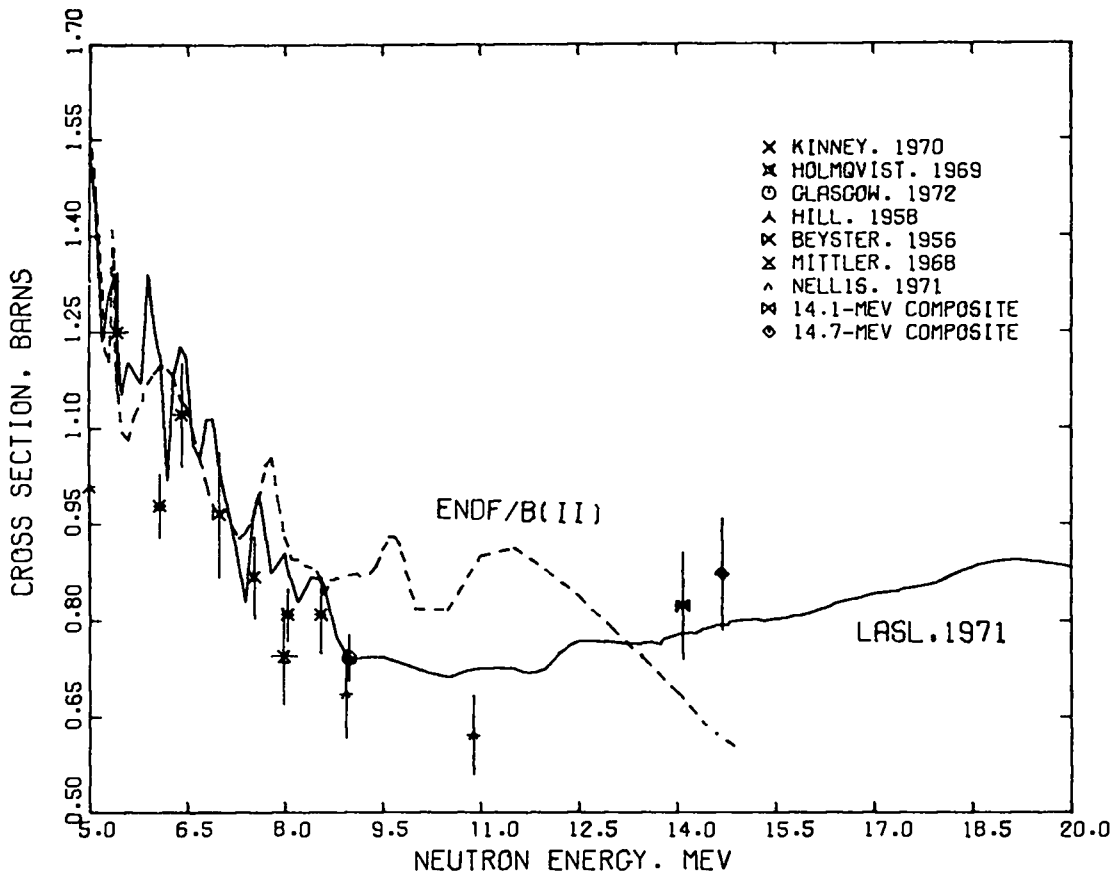


Fig. 14. Measured and evaluated elastic scattering cross section for  $^{27}\text{Al}$  from 5 to 20 MeV. The 14.1-MeV point was obtained by fitting a composite of measurements near that energy (Bo65a, Co58, Sa59, St65, Yu58); similarly, the 14.7-MeV point results from three measurements near that energy (An59, Be58, Kh58). The composites are shown in Fig. 59.

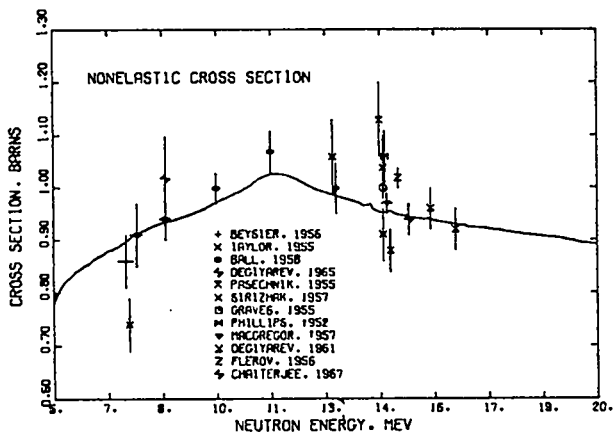


Fig. 15. Measured and evaluated nonelastic cross section for  $^{27}\text{Al}$  from 5 to 20 MeV.

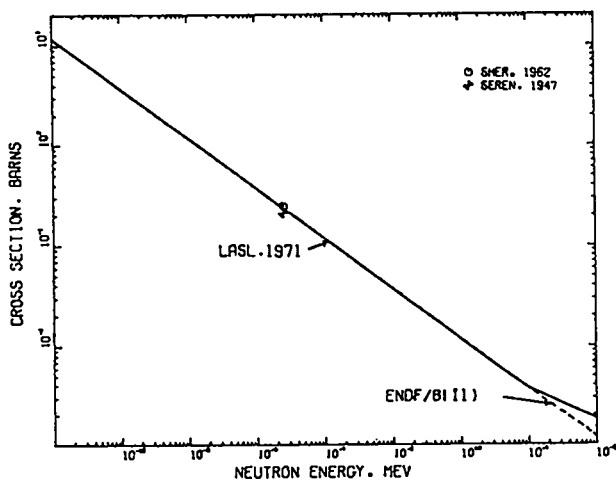


Fig. 16. Measured and evaluated  $^{27}\text{Al}(n,\gamma)^{28}\text{Al}$  cross section from  $10^{-5}$  eV to 1 keV.

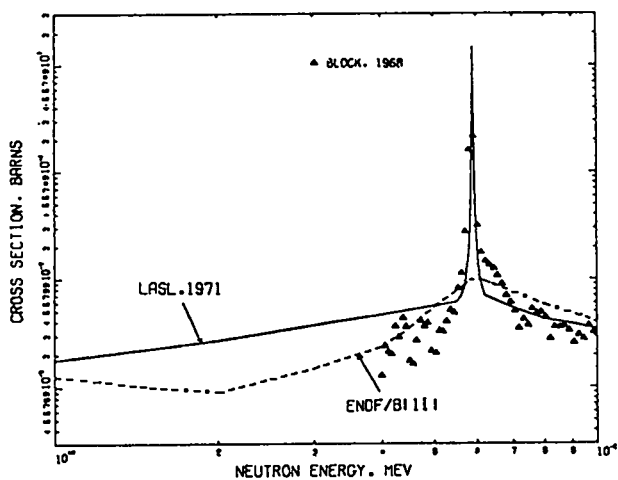


Fig. 17. Measured and evaluated  $^{27}\text{Al}(n,\gamma)^{28}\text{Al}$  cross section from 1 to 10 keV.

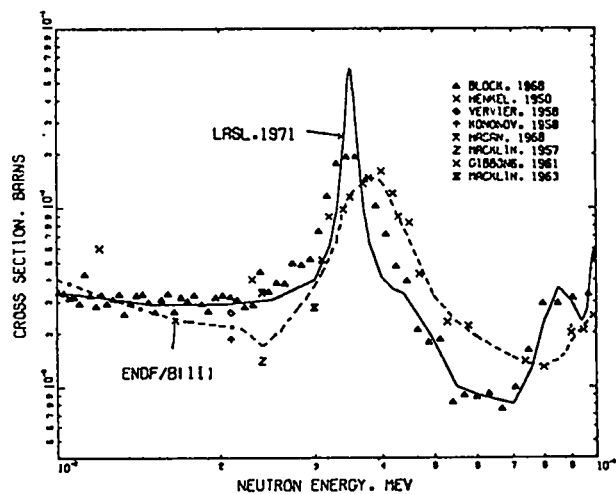


Fig. 18. Measured and evaluated  $^{27}\text{Al}(n,\gamma)^{28}\text{Al}$  cross section from 10 to 100 keV.

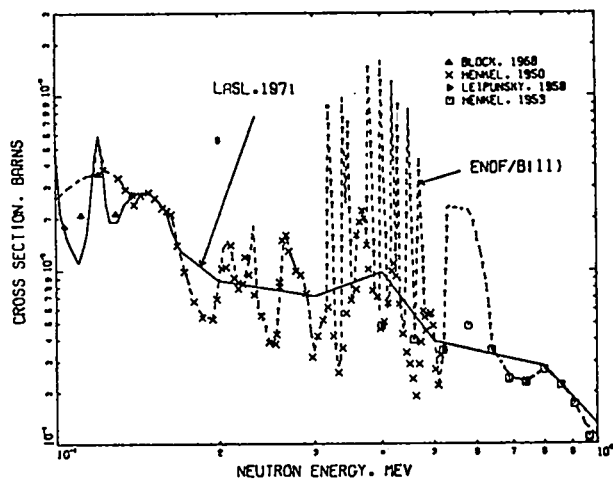


Fig. 19. Measured and evaluated  $^{27}\text{Al}(n,\gamma)^{28}\text{Al}$  cross section from 0.1 to 1.0 MeV.

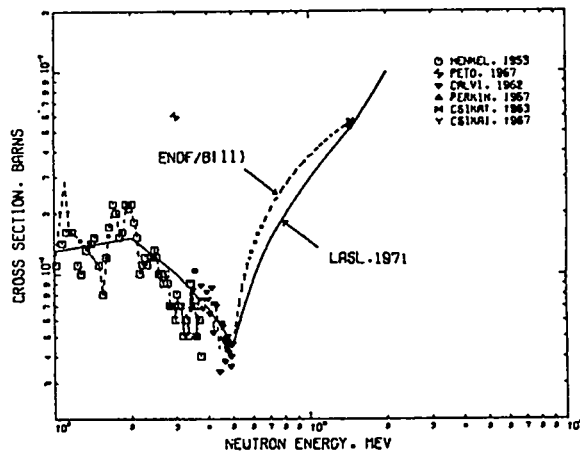


Fig. 20. Measured and evaluated  $^{27}\text{Al}(n,\gamma)^{28}\text{Al}$  cross section from 1 to 20 MeV.

14-MeV measurements (Pe57, Cs63, Cs67), which exhibit the beginning of the inverse photonuclear giant resonance.

#### 2.4. Inelastic Scattering Cross Sections

Experimental data provide the basis for the inelastic cross-section evaluation, although we used simple model calculations to supplement the measurements in certain regions. All inelastic data are given in the ENDF/B files as (n,n') reactions to discrete states; the (n,n') cross sections to the first 13 excited states of  $^{27}\text{Al}$  with  $E_x < 5$  MeV are given explicitly, whereas the data for  $E_x > 5$  MeV are grouped into 27 excitation-energy bins with bin widths of either 0.5 or 0.75 MeV.

##### 2.4.1 The $^{27}\text{Al}(n,n')$ Cross Sections for $E_x(^{27}\text{Al}) < 5$ MeV.

The level structure of  $^{27}\text{Al}$  below an excitation energy of 5 MeV is well determined and is given in Fig. 21, together with the photon branching ratios. The information in Fig. 21 was obtained mainly from the measurements of van der Leun et al. (Va67),

Elliott et al. (El68), Häusser et al. (Ha68a), Röpke et al. (Ro68, Ro69), and Huang and Ophel (Hu69), together with the 1967 compilation by Endt and van der Leun (En67).

The evaluation by Dickens (Di71) of the (n,n') cross sections to the first 13 excited states of  $^{27}\text{Al}$ , which is based on several (n,n') and (n,n' $\gamma$ ) measurements, was adopted in our evaluation for the 5- to 9-MeV energy region. For  $E_n < 5$  MeV, we mainly used the (n,n') measurements of Towle and Gilboy (To62) and Tsukada et al. (Ts61), and the (n,n' $\gamma$ ) measurements of Chung et al. (Ch68) and Mathur et al. (Ma65) to determine the cross sections. For the neutron energy region from 9 to 20 MeV, we used a smooth extrapolation of the lower energy results that passed through the 14-MeV measurements of Stelson et al. (St65) and Bonazzola et al. (Bo65a). Because the information obtained in the 14-MeV experiments (St65, Bo65a) mainly concerns states below 3-MeV excitation, we assumed roughly similar shapes for the cross sections to states with excitation energy between 3.5 and 5 MeV.

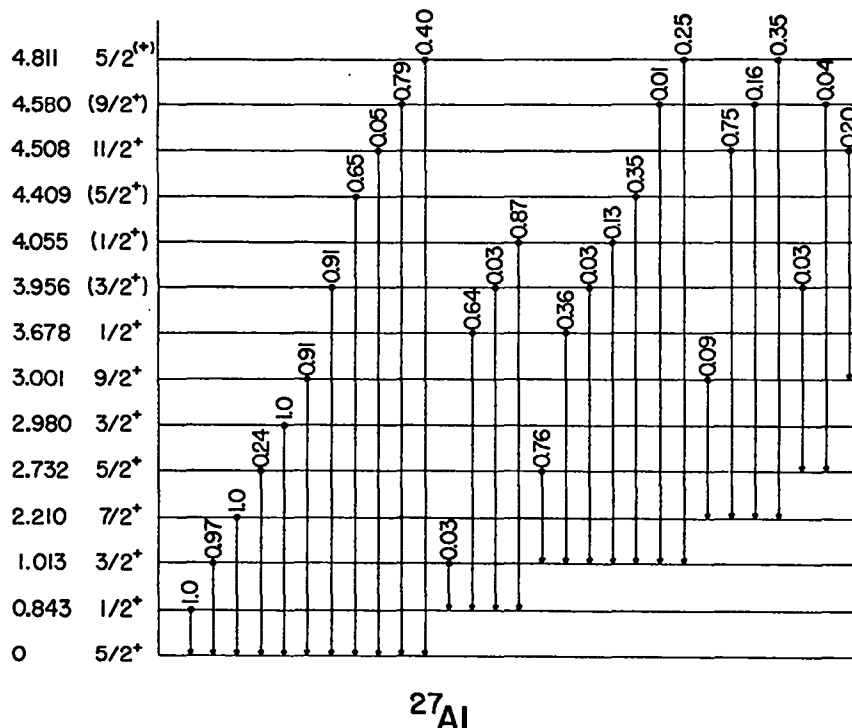


Fig. 21. Energy-level decay scheme for  $^{27}\text{Al}$ . Note that the energy scale is distorted.

The  $(n,n')$  excitation cross sections that resulted from this analysis and much of the available experimental data are shown in Figs. 22-31. Because some of the levels are too closely spaced to be clearly resolved in the measurements, we combined the excitation cross section to nearby levels in several of the figures. In all cases the shapes of the curves near threshold are based on Hauser-Feshbach calculations. The related  $(n,n'\gamma)$  measurements are described in Sec. 3.2.

#### 2.4.2 The $^{27}\text{Al}(n,n')$ Cross Sections for $E_x(^{27}\text{Al}) > 5$ MeV.

The  $(n,n')$  cross sections to states in  $^{27}\text{Al}$  with  $E_x > 5$  MeV were obtained in several steps. First, the total inelastic cross section for neutron energies above 5 MeV was estimated from direct measurements at 7 MeV by Thomson (Th63) and Towle and Owens (To67), from measurements of the ground state  $(n,n'\gamma)$  transitions between 5 and 9 MeV by Dickens (Di71), and by

subtraction of the evaluated elastic,  $(n,\gamma)$ ,  $(n,p)$ ,  $(n,d)$ ,  $(n,t)$ ,  $(n,\alpha)$ , and  $(n,2n)$  cross sections from the evaluated total cross section. The resulting total inelastic cross section, which includes the  $(n,np)$  and  $(n,n\alpha)$  reactions, is given in Fig. 32. The portion of the inelastic cross section due to states with  $E_x > 5$  MeV was then determined by subtracting the component from states with  $E_x < 5$  MeV (Sec. 2.4.1), and the remainder was distributed among the states in  $^{27}\text{Al}$  with  $E_x > 5$  MeV by using a simple evaporation model. In this calculation, the cross section was assumed to have the form

$$\sigma(E_x) \propto (E'_n - E_x) \exp(E_x/T), \quad (1)$$

where  $E'_n$  is the total center-of-mass energy available.

The nuclear temperatures used in the calculations are based approximately on  $(n,n')$  measurements by Thomson (Th63) at 7 MeV and Graves and Rosen

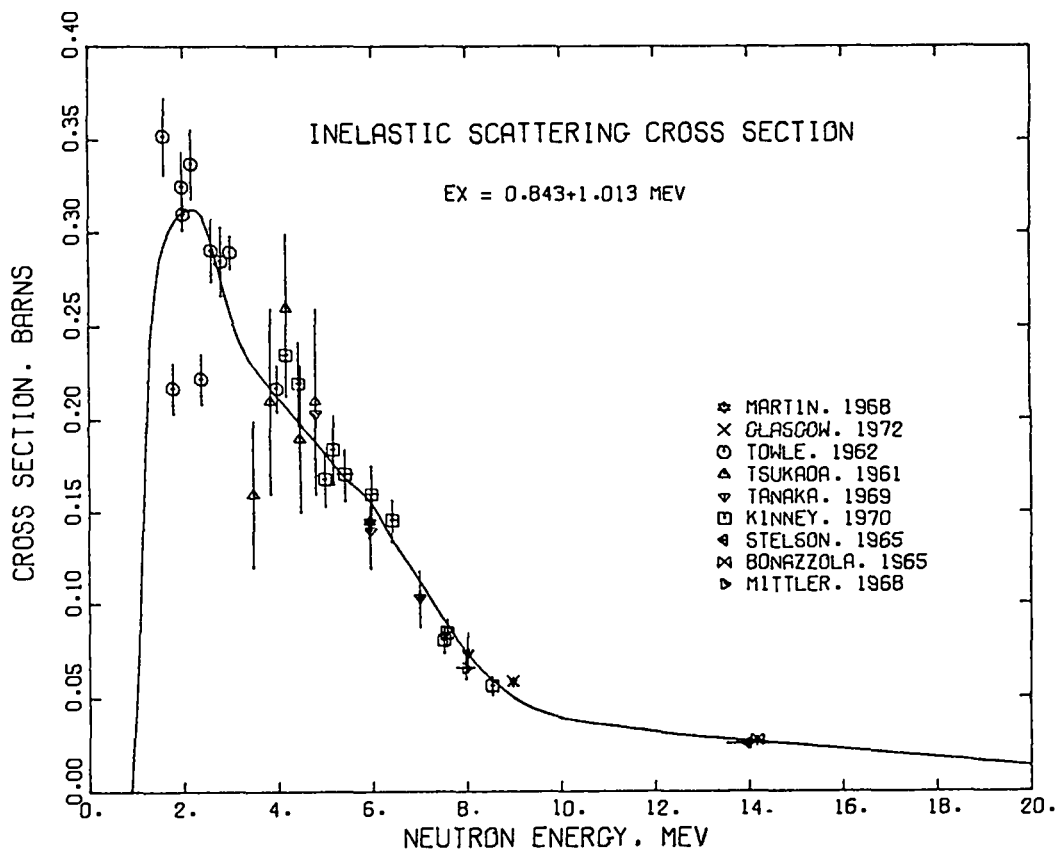


Fig. 22. Measured and evaluated inelastic-scattering cross section to the combined 0.843- and 1.013-MeV levels of  $^{27}\text{Al}$ .

(Gr53) at 14 MeV, and are given by the expression

$$T = 0.52 E_n^{0.265} \quad (\text{MeV}), \quad (2)$$

where  $E_n$  is the laboratory neutron energy in MeV. This choice of temperature also agrees with an inelastic neutron-spectrum measurement by Schectman and Anderson (Sc66) at 14 MeV for outgoing neutron energies between 1.3 and 4 MeV. If, however, the Schectman and Anderson analysis is weighted toward slightly higher secondary neutron energies, a significantly higher temperature (1.9 MeV) results, indicating that the simple evaporation model used here might underestimate the cross section for higher energy inelastic neutrons.

The  $(n,n')$  cross sections for  $E_x > 5$  MeV that resulted from the above analysis are represented in the ENDF/B files as excitation cross sections to 27 fictitious levels in  $^{27}\text{Al}$  with excitation energies between 5.25 and 18.875 MeV. Each of these "levels" represents a bin or group of levels over a range of excitation energies. Bin widths of 0.5 MeV are used for  $E_x < 17$  MeV and widths of 0.75 MeV for higher ex-

citation energies. This treatment as quasi-discrete levels allows the energy-angle relationships of outgoing neutrons to be preserved in a very simple manner; in particular, it preserves the forward peaking in the laboratory system of the lower-energy secondary neutrons caused by center-of-mass motion.

2.5 The  $^{27}\text{Al}(n,np)^{26}\text{Mg}$ ,  $^{27}\text{Al}(n,n\alpha)^{23}\text{Na}$ , and  $^{27}\text{Al}(n,2n)^{26}\text{Al}$  Cross Sections

The thresholds for the  $(n,np)$ ,  $(n,n\alpha)$ , and  $(n,2n)$  reactions on  $^{27}\text{Al}$  are 8.58, 10.48, and 13.54 MeV, respectively. Very little information is available on these reactions, and the evaluated curves described here are little more than rough estimates in some regions.

Measured values of the  $(n,np)$  cross section near 14 MeV vary from 17 mb (Ha62) to 200 mb (G161), with several intermediate results (A157, A161). Information on this cross section is also available from gamma-ray production measurements for the 1.809-MeV photon, which results from de-excitation of the first excited state in  $^{26}\text{Mg}$ . Many of the higher states in

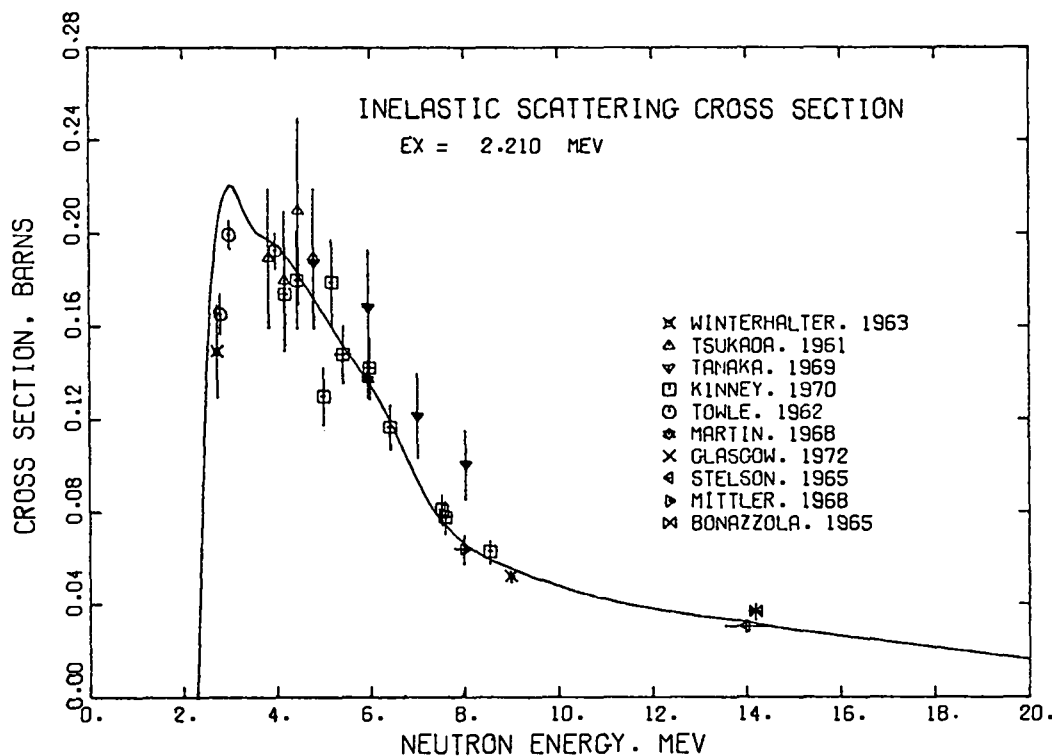


Fig. 23. Measured and evaluated inelastic-scattering cross section to the 2.210-MeV level of  $^{27}\text{Al}$ .

$^{26}\text{Mg}$  cascade through the 1.809-MeV level, as is shown in the level diagram of Fig. 33 (En67), so that the production cross section for the 1.809-MeV photon gives a lower limit for the (n,np) cross section, after correction for the (n,d) reaction. The evaluated (n, $\gamma$ ) cross section for the 1.809-MeV photon is 112 mb at 14 MeV, as is described in Sec. 3.2.1. Our evaluated (n,np) cross section at that energy is approximately 160 mb.

The (n,np) and (n,n $\alpha$ ) cross sections, together with the total (n,n'), the (n,n $\gamma$ ), and the (n,2n) cross sections are shown in Fig. 34. The (n,n' $\gamma$ ) cross section is the sum of (n,n') reactions to states in  $^{27}\text{Al}$  that decay by gamma emission, and the total (n,n') is the sum of the (n,n $\gamma$ ), (n,np), and (n,n $\alpha$ ) cross sections. Because there is no experimental information available on the (n,n $\alpha$ ) cross section, the curve in Fig. 34 is only a rough estimate.

The only direct information on the (n,2n) cross section comes from activation measurements (Ma60, Cs63) involving the isomeric first excited state of  $^{26}\text{Al}$  at excitation energy 229 keV. Because many photon transitions in  $^{26}\text{Al}$  bypass this state (En67), the activation measurements furnish only a lower limit for the (n,2n) cross section. The evaluated curve shown in Fig. 34 is based roughly on the assumption that highly-excited states in  $^{27}\text{Al}$  decay 50% by neutron emission. The (n,2n) cross section that results at 20 MeV is slightly more than twice the measured

value for production of the metastable state. This value appears reasonable, but it is only a rough estimate.

The evaluated (n,2n) cross section is entered as a separate reaction in the ENDF/B files. The (n,np) and (n,n $\alpha$ ) cross sections are not entered explicitly, but are included by flagging the (n,n')

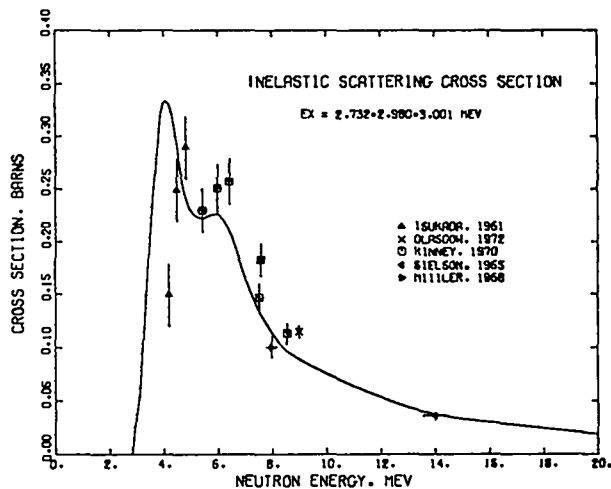


Fig. 25. Measured and evaluated inelastic-scattering cross section to the combined 2.732-, 2.980- and 3.001-MeV levels of  $^{27}\text{Al}$ .

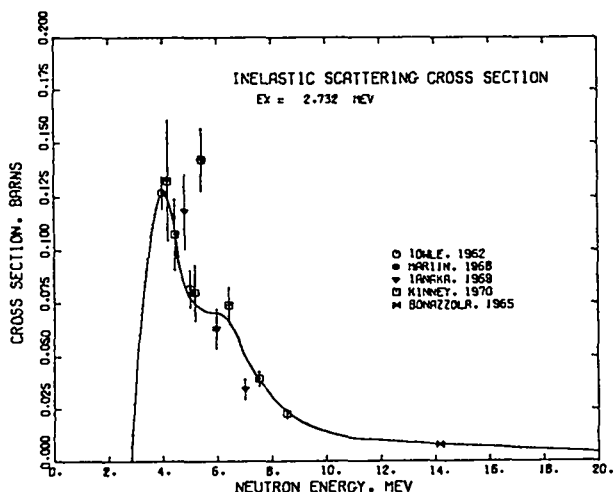


Fig. 24. Measured and evaluated inelastic-scattering cross section to the 2.732-MeV level of  $^{27}\text{Al}$ .

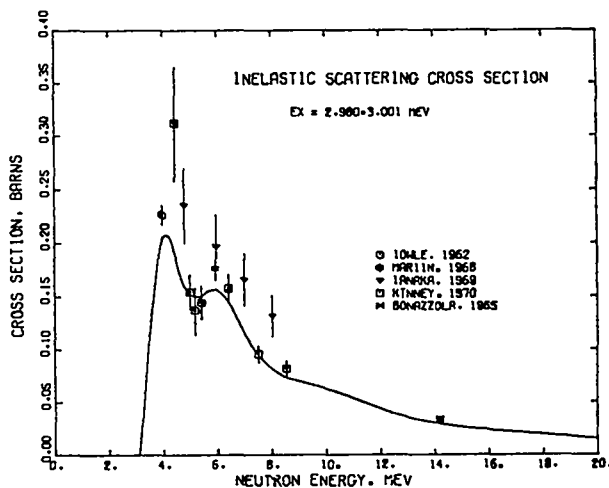


Fig. 26. Measured and evaluated inelastic-scattering cross section to the combined 2.980- and 3.001-MeV levels of  $^{27}\text{Al}$ .

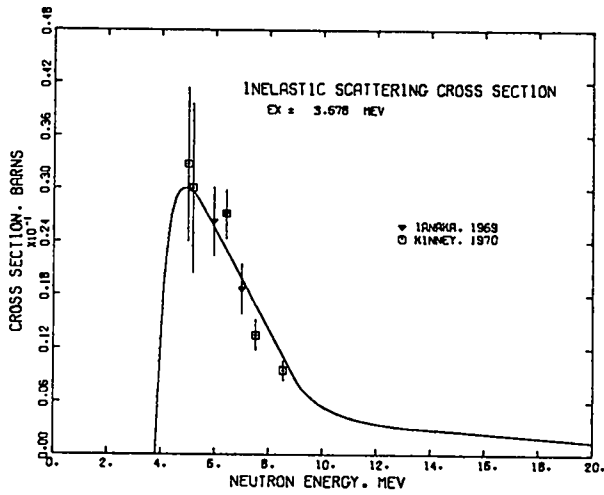


Fig. 27. Measured and evaluated inelastic-scattering cross section to the 3.678-MeV level of  $^{27}\text{Al}$ .

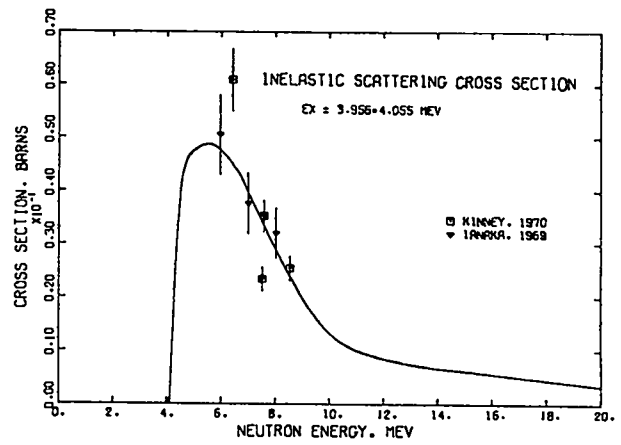


Fig. 29. Measured and evaluated inelastic-scattering cross section to the combined 3.956- and 4.055-MeV levels of  $^{27}\text{Al}$ .

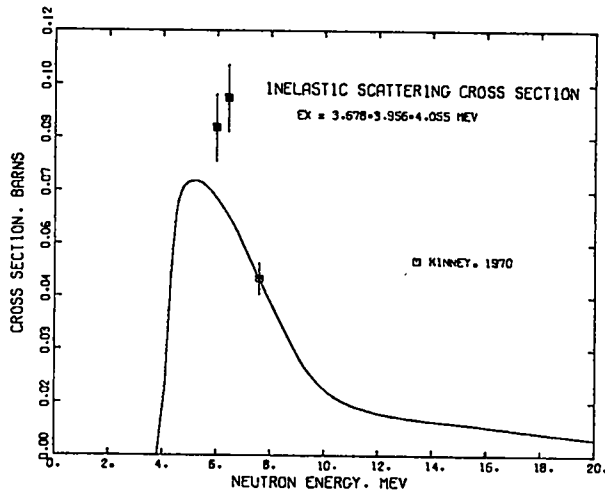


Fig. 28. Measured and evaluated inelastic-scattering cross section to the combined 3.678-, 3.956-, and 4.055-MeV levels of  $^{27}\text{Al}$ .

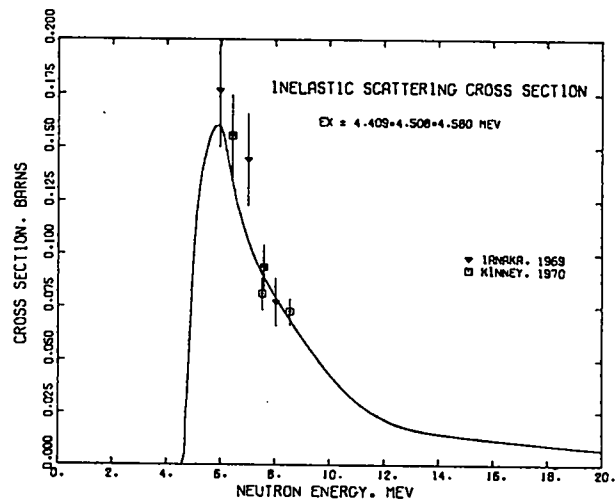


Fig. 30. Measured and evaluated inelastic-scattering cross section to the combined 4.409-, 4.508-, and 4.580-MeV levels of  $^{27}\text{Al}$ .

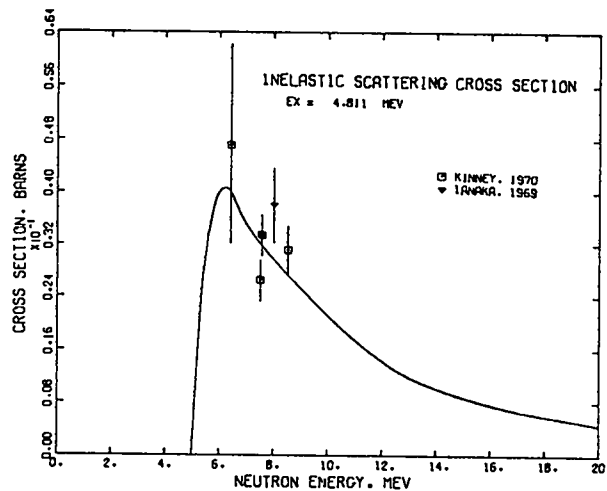


Fig. 31. Measured and evaluated inelastic-scattering cross section to the 4.811-MeV level of  $^{27}\text{Al}$ .

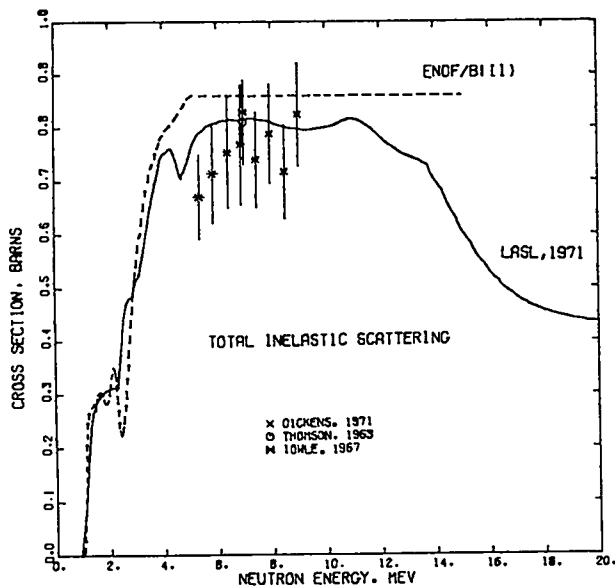


Fig. 32. Measured and evaluated total inelastic-scattering cross section for  $^{27}\text{Al}$ . The  $(n,np)$  and  $(n,n\alpha)$  reactions are included.

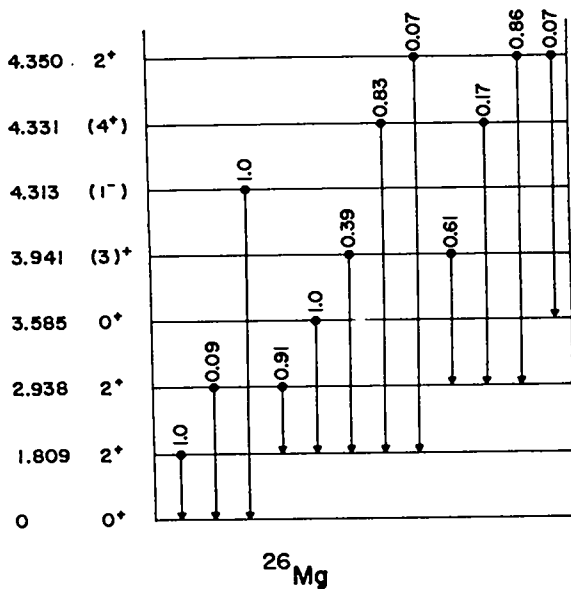


Fig. 33. Energy-level decay scheme for  $^{26}\text{Mg}$ . Note that the energy scale is distorted.

reactions to certain higher-excitation states in  $^{27}\text{Al}$  as decaying by proton or alpha emission. This representation assumes a sequence in the reactions that is only partially true; however, it should cause no difficulty in most practical problems, and it allows the energy-angle relationship of secondary neutrons to be better preserved in the laboratory system.

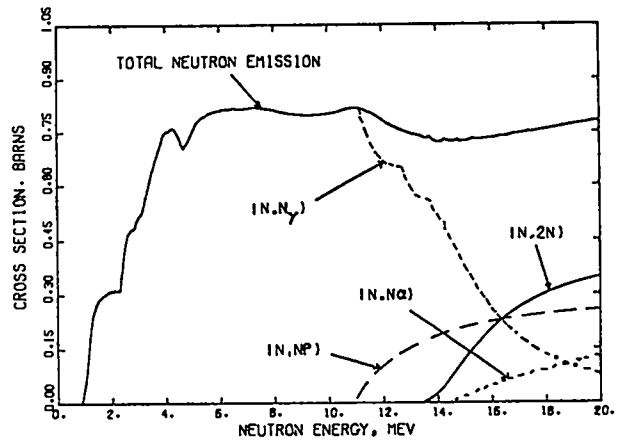


Fig. 34. The total neutron-emission cross section compared to its constituent  $(n,n')$ ,  $(n,np)$ ,  $(n,n\alpha)$ , and  $(n,2n)$  reactions. The  $(n,n')$  curve is defined as that part of the  $(n,n')$  cross section which results in photon emission.

### 2.6 The $^{27}\text{Al}(n,p)^{27}\text{Mg}$ Cross Section

The threshold for the  $(n,p)$  reaction with  $^{27}\text{Al}$  occurs at 1.90 MeV. For neutron energies below 5 MeV, we adopted an earlier evaluation by Joanou and Stevens (Jo64), which was also used for ENDF/B(II). Above 5 MeV, the recommended curve is based on measurements that use the 9.5-min  $\beta^-$  activity of  $^{27}\text{Mg}$ .

The evaluated curve is compared to the available measurements between threshold and 7 MeV in Fig. 35, between 7 and 13 MeV in Fig. 36, and between 13 and 20 MeV in Fig. 37. The results of Ferguson and Albergotti (Fe67), which are substantially lower than the evaluation in Figs. 36 and 37, are from a relative measurement that was normalized to a value of 55 mb near 13 MeV. Similarly, absolute data were obtained at only one energy (50 mb at 14.4 MeV) in the Gabbard and Kern measurement (Ga62), which also lies well below the evaluation, and the remaining Gabbard points were normalized to that value. Therefore, because the preponderance of experimental data near 14 MeV suggest a substantially higher  $(n,p)$  cross section, we chose the evaluated curve to follow approximately the measurements of Mani (Ma60), resulting in a cross section of 77 mb at 14.1 MeV.

### 2.7 The $^{27}\text{Al}(n,d)^{26}\text{Mg}$ and $^{27}\text{Al}(n,t)^{25}\text{Mg}$ Cross Sections

The thresholds for the  $^{27}\text{Al}(n,d)$  and  $^{27}\text{Al}(n,t)$  reactions are 6.27 and 11.29 MeV, respectively. Because only one measurement is available for the  $(n,d)$  reaction, we assumed that the cross section has about the same shape as the  $(n,p)$  cross section. The re-

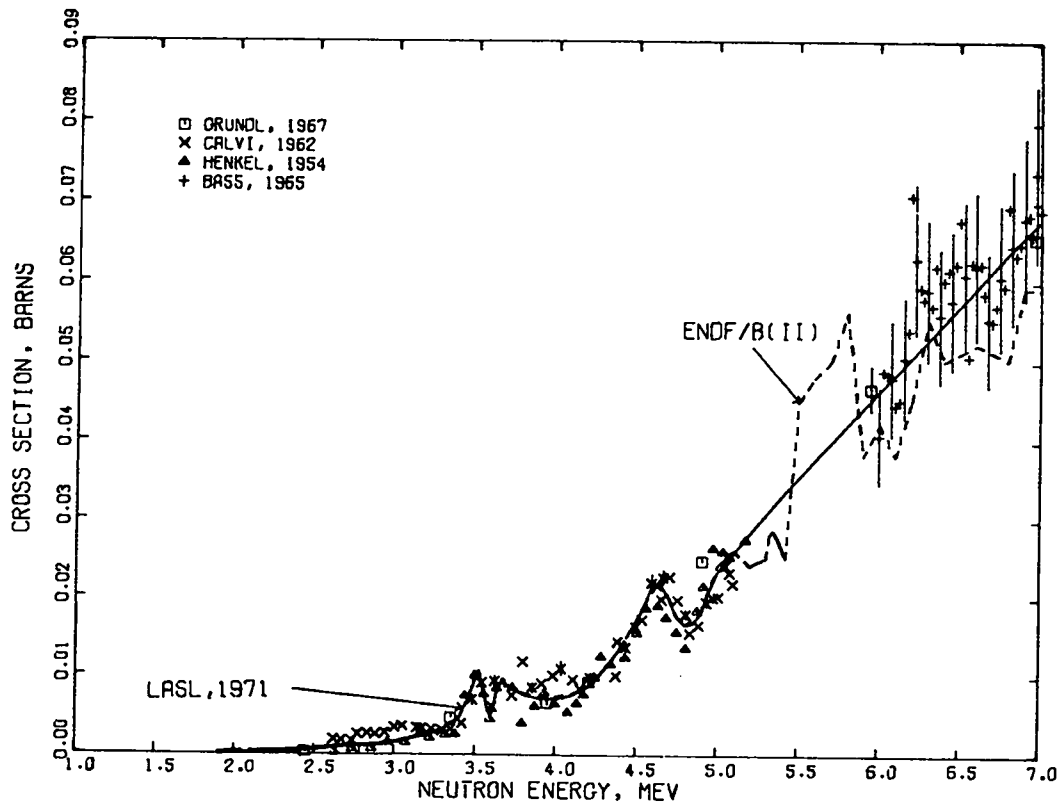


Fig. 35. Measured and evaluated  $^{27}\text{Al}(n,p)^{27}\text{Mg}$  cross section from 1 to 7 MeV.

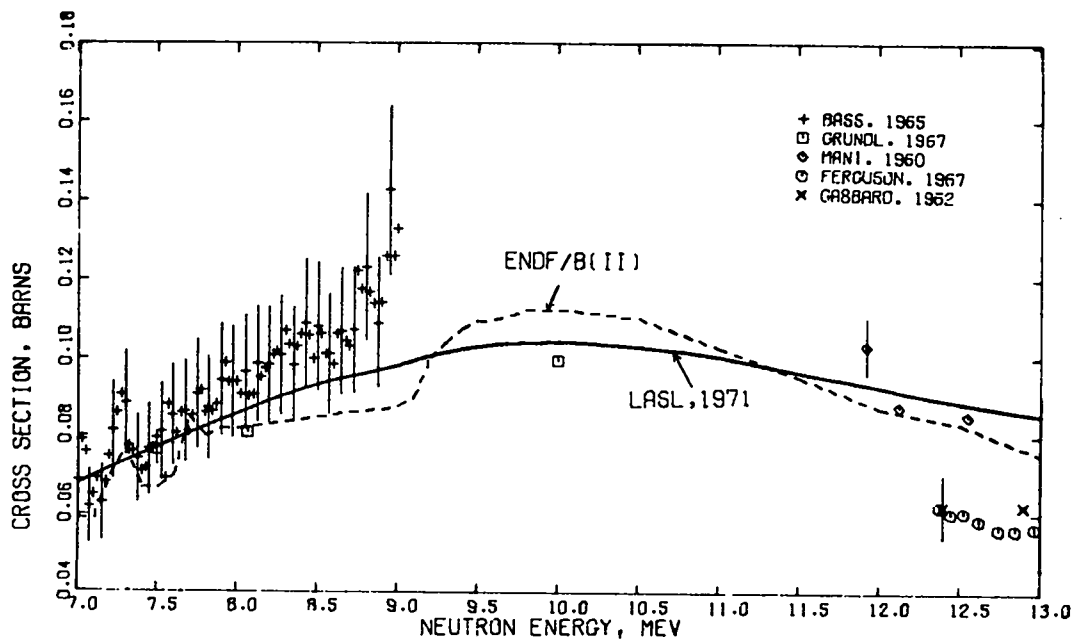


Fig. 36. Measured and evaluated  $^{27}\text{Al}(n,p)^{27}\text{Mg}$  cross section from 7 to 13 MeV.

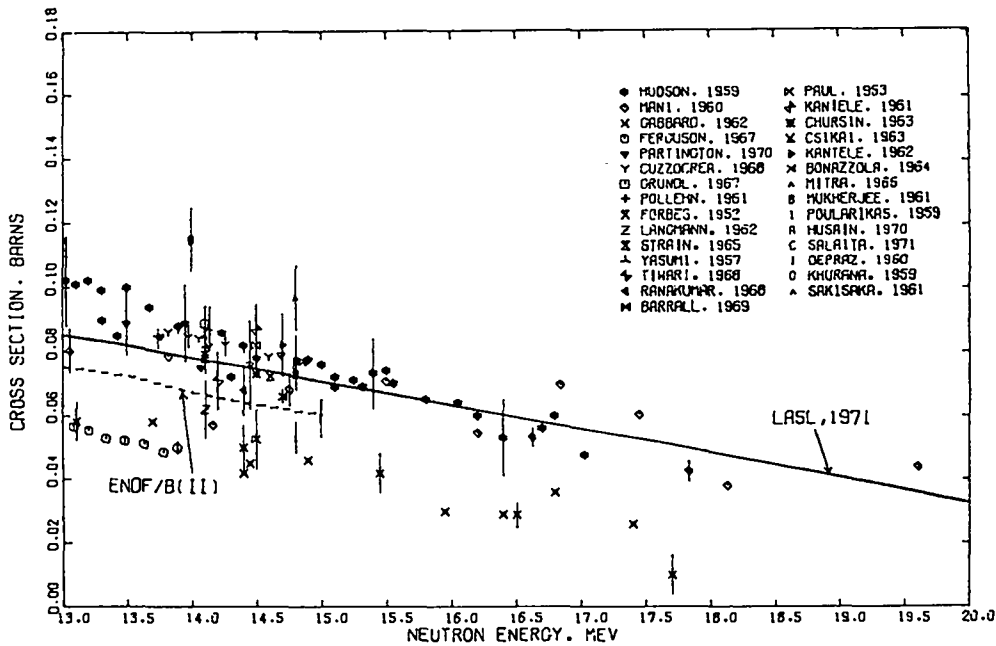


Fig. 37. Measured and evaluated  $^{27}\text{Al}(n,p)^{27}\text{Mg}$  cross section from 13 to 20 MeV.

sulting curve was normalized to the lone measurement by Glover and Weigold (G161) at 14.8 MeV, as shown in Fig. 38. There are no measurements available for the (n,t) reaction, so we assumed the same shape for the (n,t) cross section as was used for the (n,d) cross section, with an appropriate shift in energy. The evaluated (n,t) curve, also shown in Fig. 38, reaches a maximum of 15 mb at 20 MeV.

#### 2.8 The $^{27}\text{Al}(n,\alpha)^{24}\text{Na}$ Cross Section

The  $^{27}\text{Al}(n,\alpha)$  reaction forms  $^{24}\text{Na}$  which  $\beta^-$  decays to  $^{24}\text{Mg}$  with a 15-h half-life. Consequently, a large number of cross-section measurements are available from activation studies. Although the threshold for the reaction is 3.25 MeV, the cross section does not become important until above 6 MeV. The evaluated curve between 5 and 12.5 MeV is compared to the available measurements and to the ENDF/B(II) curve in Fig. 39. Our results lie below the ENDF/B(II) data at these energies and represent somewhat of a compromise between the measurements of Butler and Santry (Bu63) and Tewes et al. (Te60). It is interesting to note that if the Tewes data are renormalized by a factor of 1.37, very good agreement with the Butler data is obtained.

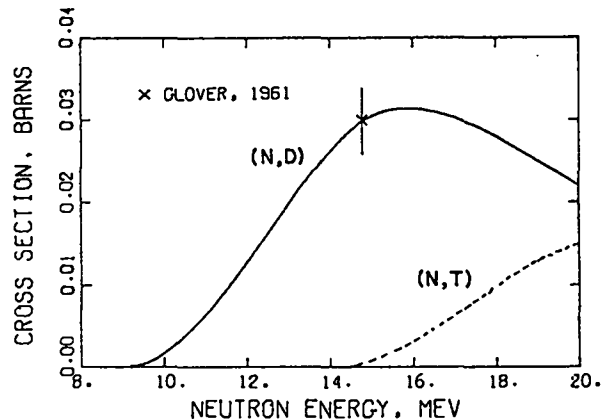


Fig. 38. Evaluated  $^{27}\text{Al}(n,d)^{26}\text{Mg}$  and  $^{27}\text{Al}(n,t)^{25}\text{Mg}$  cross sections compared to the (n,d) measurement by Glover (G161).

Figure 40 shows the measured and evaluated (n, $\alpha$ ) cross section from 12.5 to 20 MeV. The evaluated result is 124 mb at 14 MeV. Past 14 MeV, the curve is well determined and is based mainly on the data of Butler and Santry (Bu63) and Paulsen and Liskien (Pa65).

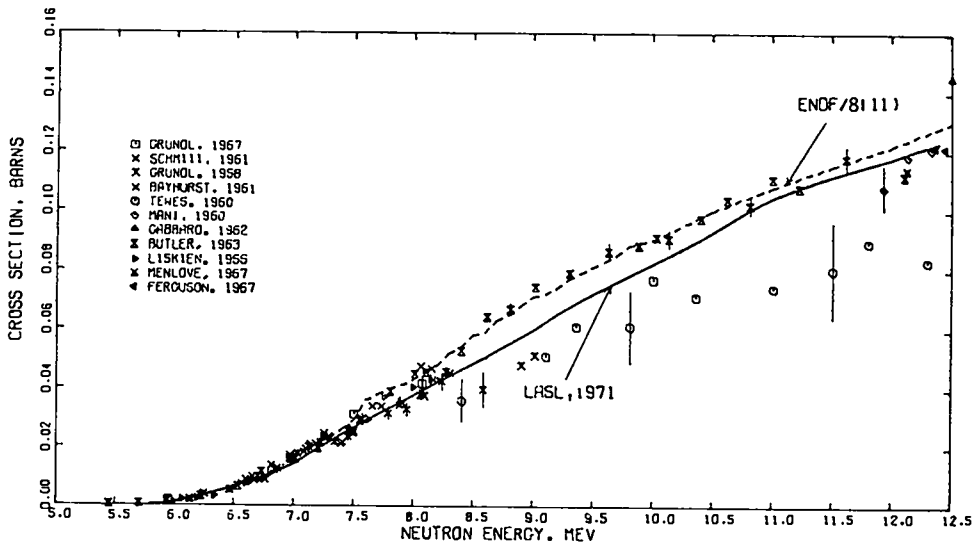


Fig. 39. Measured and evaluated  $^{27}\text{Al}(n,\alpha)^{24}\text{Na}$  cross section from 5.0 to 12.5 MeV.

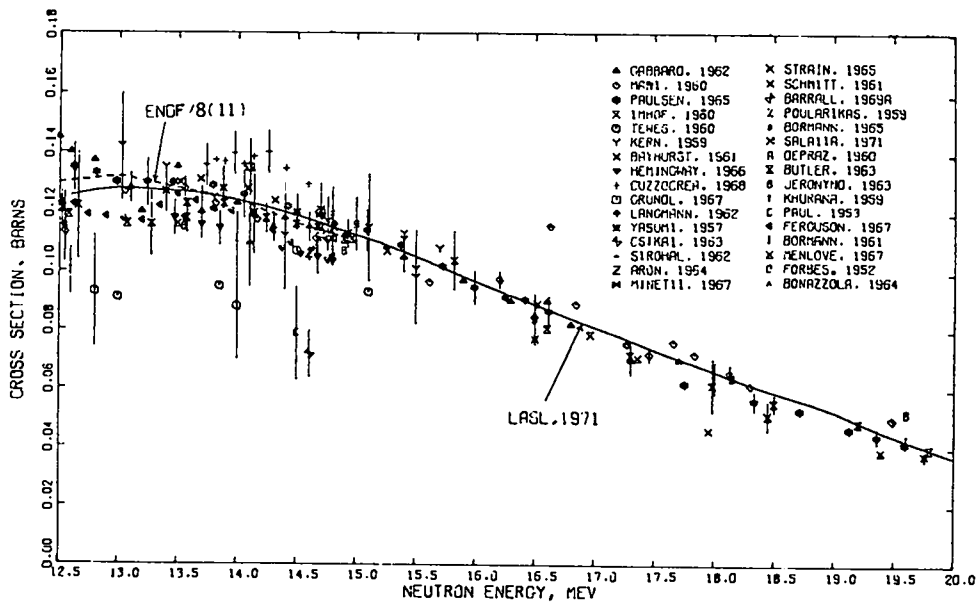


Fig. 40. Measured and evaluated  $^{27}\text{Al}(n,\alpha)^{24}\text{Na}$  cross section from 12.5 to 20 MeV.

### 3. PHOTON-PRODUCTION CROSS SECTIONS AND ENERGY SPECTRA

#### 3.1 Photon Production from the $^{27}\text{Al}(n,\gamma)^{28}\text{Al}$ Reaction

In the absence of data at epithermal neutron energies, we assumed that the photon energy spectrum resulting from radiative capture of thermal neutrons applies at all neutron energies for the (n,γ) reac-

tion. In evaluating the thermal spectrum, we took the energies of the prominent photons primarily from the measurements of Orphan et al. (Or70), and relied mainly on the compilation by Bartholomew et al. (Ba67) for the photon intensities. Preliminary low-background measurements on a very pure sample by Journey (Ju71) were also used in evaluating the intensities.

The Journey results indicate that several of Orphan's strong lines below 1 MeV are spurious, and consequently these were omitted from the evaluation.

In addition to the strong lines, a continuum of gamma rays was included in the evaluation based on the weak lines and unresolved continuum given by Orphan et al. (Or70). The intensity of the continuum was normalized to bring the total energy per capture up to the binding energy of  $^{28}\text{Al}$ . Table II lists the composite photon spectrum (lines plus continuum) grouped into 0.5-MeV bins, together with spectra measured by seven previous authors. The total photon multiplicity for the evaluated spectrum is 2.035 photons/capture. The last four columns in Table II agree semi-quantitatively except at the lowest energies. The large multiplicity in the lowest energy bin for the evaluation results mainly from the extremely intense 30.6-keV photon from the first excited state of  $^{28}\text{Al}$ (Ju71). Unfortunately, we did not become aware of the measurement by Hardell et al. (Ha69) given in Table II until after the evaluation. We plan to incorporate those results into the evaluation at a future date.

### 3.2. Photon Production from $^{27}\text{Al}(n,xy)$ Reactions

Inelastic scattering is the dominant source of photons in the MeV neutron energy region. The three classes of inelastic gamma rays that we considered are discrete photons resulting from excitation of states in  $^{27}\text{Al}$  with  $E_x < 5$  MeV, discrete photons resulting from cascades to levels below 5 MeV from higher states in a continuum or unresolved region, and transitions completely within the continuum region, defined here to be states in  $^{27}\text{Al}$  with  $E_x > 5$  MeV. Contributions from the first two classes of transitions are described in Sec. 3.2.1, and the third class is described in Sec. 3.2.2. In addition to photons from inelastic scattering, photons from  $(n,p\gamma)$ ,  $(n,np\gamma)$ , and  $(n,2n\gamma)$  reactions are also included in the evaluation.

#### 3.2.1 Discrete Photons from $^{27}\text{Al}(n,xy)$ Reactions

The photons from inelastic scattering to levels in  $^{27}\text{Al}$  with  $E_x < 5$  MeV are included explicitly in the evaluation. The cross section for these discrete photons was calculated below  $E_n = 5$  MeV from the evaluated  $(n,n')$  excitation cross sections, together

TABLE II  
CAPTURE GAMMA-RAY SPECTRUM OF  $^{27}\text{Al}$  FOR THERMAL NEUTRONS IN  
PHOTONS/100 CAPTURES

Photon Energy Bin (MeV)	Bartholomew 1958 <sup>a</sup>	Groshev 1959 <sup>a</sup>	Draper 1963 <sup>a</sup>	Greenwood 1965 <sup>a</sup>	Hardell 1969	Maerker 1969	Orphan 1970	Present Results
0 - 0.5					0.5		12.6	27.5
0.5 - 1.0				9.2	2.3	6.1	10.5	10.3
1.0 - 1.5			7.7	4.9	3.3	12.5	0.8	2.5
1.5 - 2.0			5.4	4.3	7.0	10.4	6.5	7.9
2.0 - 2.5		8.1	13.0	8.8	10.8	13.1	12.9	12.8
2.5 - 3.0	4.6	15.0	10.0		20.0	20.5	13.4	18.6
3.0 - 3.5	13.5	10.9	17.0		17.3	15.9	10.7	13.9
3.5 - 4.0	6.9	11.8	7.0		13.6	14.3	11.1	16.5
4.0 - 4.5	10.7	13.1	15.0		16.3	16.1	15.0	19.5
4.5 - 5.0	7.6	15.4	16.0		18.8	17.6	16.1	20.3
5.0 - 5.5	3.3	5.5			6.5	6.8	5.4	9.5
5.5 - 6.0	2.5	0.8			2.3	2.8	1.3	1.7
6.0 - 6.5	3.4	5.3			6.4	6.0	4.5	7.9
6.5 - 7.0	1.5	1.7			1.5	2.2	4.0	5.3
7.0 - 7.5	0.5	.			0.1	0.7	2.7	3.0
7.5 - 8.0	20.0	24.0	32.0	37.0	33.0	32.4	29.7	26.5
% Binding Energy	50	69	71	42	93	96	84	100

<sup>a</sup>Taken from the compilation by Bartholomew et al. (Ba67).

with the level decay scheme given in Fig. 21 (Sec. 2.4.1). Above  $E_n = 5$  MeV, however, the second and third classes of transitions described above become possible, and a calculation based on statistical theory was made to estimate these continuum contributions. The calculation yielded estimates of continuous photon-energy spectra (given in Sec. 3.2.2) as well as contributions from the continuum states to the discrete photons that are associated with the resolved states below  $E_x = 5$  MeV.

The statistical theory calculations were performed with the code SPECT10, using a method similar to that described by Troubetzkoy (Tr61). For a given incident neutron energy, the probability of exciting states of excitation energy  $E_x$  in the residual nucleus ( $^{27}\text{Al}$ ) by neutron emission from the compound state ( $^{28}\text{Al}$ ) was assumed to have the form

$$N_n \Delta E_x \propto (E_{\text{max}} - E_x) \sigma_{\text{inv}}(E_x) \rho(E_x), \quad (3)$$

where  $E_{\text{max}}$  is the maximum energy available in the center-of-mass system,  $\sigma_{\text{inv}}(E_x)$  is the inverse cross section for the transition, and  $\rho(E_x)$  is the density of states at energy  $E_x$  in the residual nucleus. The decay by photon emission of states in the residual nucleus was assumed to be described by

$$N_\gamma(E_x, E'_x) \Delta E_x \propto (E_x - E'_x)^{2\ell+1} \rho(E'_x), \quad (4)$$

where  $E_x$  and  $E'_x$  are the excitation energies of the initial and final states, respectively, and  $\ell$  is the multipole order of the transition.

For the  $(n, n'\gamma)$  calculations, a level density expression of the form

$$\rho(E_x) \propto \exp(E_x/T) \quad (5)$$

was included with the same temperatures,  $T$ , as were used in the  $(n, n')$  cross section evaluation in Eq. (2), Sec. 2.4.2. The inverse cross section was taken to be constant, and pure dipole transitions ( $\ell=1$ ) were assumed. We determined the normalization of the calculations by the total inelastic cross section. Transitions entirely within the continuum region were assumed to be independent of spin. However, in calculating the population of discrete levels due to transitions from the continuum region, the number of states of spin  $J$  at a particular energy in the con-

tinuum was assumed proportional to  $(2J+1) \exp(-J(J+1)/2\sigma^2)$ , where  $\sigma$  is a spin cutoff factor related to the excitation energy and nuclear moment of inertia. Transitions from states in the continuum were allowed to proceed by dipole radiation to the eligible discrete states, and the discrete states were de-excited by the decay scheme shown in Fig. 21.

A summary of the discrete photon transitions from  $(n, n')$  reactions that were included in the evaluation is given in Table III. These transitions are from  $^{27}\text{Al}$  states with  $E_x < 5$  MeV and result from the decay scheme shown in Fig. 21. The evaluated curves for a selection of discrete gamma rays are compared to the available experimental data in Figs. 41-50. Anisotropies in the photon angular distributions are small (Sec. 5.3). Often the experimental results at a single angle ( $\mu = \cos\theta$ ) have simply been multiplied by  $4\pi$  steradians for the comparisons shown in Figs. 41-50. Where integral results are available, the " $\mu$ " entry in the figures is left blank.

TABLE III  
GAMMA RAYS FROM INELASTIC SCATTERING

$E_\gamma$ (MeV)	$E_i$ (MeV)	$E_f$ (MeV)
4.811	4.811	0.
4.580	4.580	0.
4.508	4.508	0.
4.409	4.409	0.
3.956	3.956	0.
3.798	4.811	1.013
3.567	4.580	1.013
3.396	4.409	1.013
3.212	4.055	0.843
3.113	3.956	0.843
3.042	4.055	1.013
3.001	3.001	0.
2.980	2.980	0.
2.943	3.956	1.013
2.835	3.678	0.843
2.732	2.732	0.
2.665	3.678	1.013
2.601	4.811	2.210
2.370	4.580	2.210
2.298	4.508	2.210
2.210	2.210	0.
1.848	4.580	2.732
1.719	2.732	1.013
1.507	4.508	3.001
1.224	3.956	2.732
1.013	1.013	0.
0.843	0.843	0.
0.791	3.001	2.210
0.170	1.013	0.843

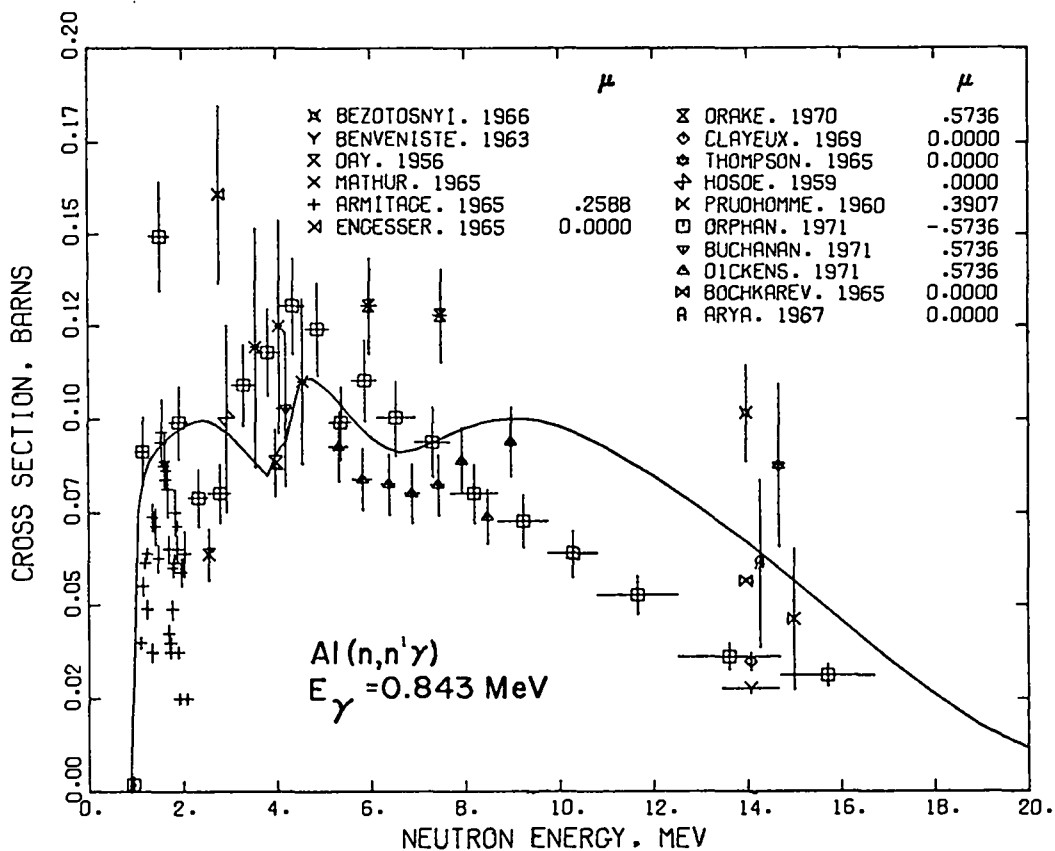


Fig. 41. Measured and evaluated  $^{27}\text{Al}(n,n'\gamma)$  cross section for the 0.843-MeV photon from the  $0.843 \rightarrow 0$ -MeV transition in  $^{27}\text{Al}$ .

The measurements by Dickens (Di71), Orphan and Hoot (Or71), Buchanan et al. (Bu71), Nyberg et al. (Ny69), Clayeux and Grenier (Cl69), and Chung et al. (Ch68) were made with Ge(Li) detectors and have much better energy resolution than the older measurements that were made with scintillation detectors, mainly NaI. In Figs. 45-47, only Ge(Li) measurements are shown because a nearby gamma ray was not resolved in the NaI measurements. Similarly, the sum of the 2.980- and 3.001-MeV photons that is shown in Fig. 48 is compared only to scintillation detector measurements, which did not resolve these gamma rays.

As described earlier, the photon-production cross sections below  $\sim 5$  MeV are based on the  $(n,n')$  level-excitation cross sections. Above 5 MeV, the cross sections contain calculated contributions from levels with  $E_x > 5$  MeV. We adjusted the calculated contributions for the 0.843-, 2.732-, 2.980-, 3.001-, 3.965-, and 4.055-MeV levels to produce bet-

ter agreement with the measurements by Dickens (Di71) from 5 to 9 MeV and with several 14-MeV results (Ar67, Be63, Be66, Bo65, Cl69, Ny69, Pr60, Th65). The measurements by Orphan and Hoot (Or71) at Gulf Radiation Technology (GRT) that are included in Figs. 41-50 did not become available until after the evaluation was completed. There is significant disagreement between the evaluated curves and the Orphan data for several of the photons, with the evaluation generally being too high in the 8- to 14-MeV region. However, the GRT results are also lower than several of the 14-MeV measurements, which partially accounts for the discrepancy with the evaluation. The results of Figs. 41-50 indicate that the simple calculation described above generally over-estimates the contribution from unresolved states to the discrete-photon cross sections.

The thresholds for the  $^{27}\text{Al}(n,np\gamma)$  and  $^{27}\text{Al}(n,2n\gamma)$  reactions are 10.46 and 13.98 MeV, respectively. The

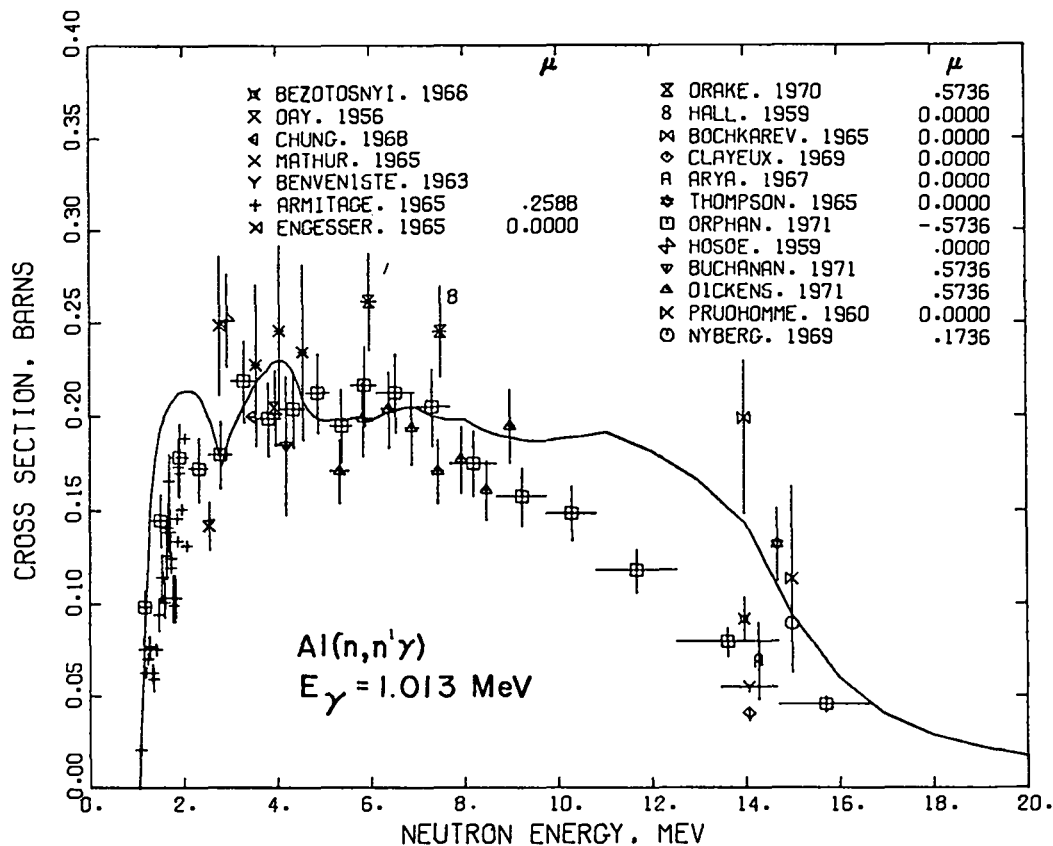


Fig. 42. Measured and evaluated  $^{27}\text{Al}(n,n'\gamma)$  cross section for the 1.013-MeV photon from the 1.013  $\rightarrow$  0-MeV transition in  $^{27}\text{Al}$ .

photon-production cross sections and energy spectra from these reactions were also estimated in the statistical theory calculations described above. These estimates were made by assuming that states in  $^{27}\text{Al}$  above the threshold for particle emission (8.271 MeV) decay predominantly by particle emission. For the (n,np) reaction, rough account of penetrability effects on the outgoing proton was taken using the  $\sigma_{\text{inv}}$  factor in Eq. (3). Above the threshold for the (n,2n) reaction, the additional assumption was made that states in  $^{27}\text{Al}$  at high excitation energy decay 50% by proton emission and 50% by neutron emission. The calculated cross sections and energy spectra from the (n,np) and (n,2n) reactions were appropriately normalized with the evaluated (n,np) and (n,2n) cross sections.

Because the threshold for the (n,2n) reaction is very high and the cross section so uncertain, we combined our estimates for this reaction with the

(n,n' $\gamma$ ) data in the ENDF/B files. However, the evaluated photon-production cross sections for the  $^{27}\text{Al}(n,\text{np})^{26}\text{Mg}$  reaction are included explicitly, and a summary of the discrete photons from this source is given in Table IV. The decay scheme for  $^{26}\text{Mg}$  is given in Fig. 33. The evaluated curve for the 1.809-MeV photon from the first excited state of  $^{26}\text{Mg}$  is shown in Fig. 51. The (n,np) cross section was adjusted as noted in Sec. 2.5 to produce agreement with the experiments shown in Fig. 51. In Fig. 52, the sum of the evaluated curves for the 1.719- and 1.809-MeV photons is compared to the measurements near 14-MeV, which did not resolve the two photons. Below 10 MeV, the curve is due entirely to the 1.719-MeV transition, which results from inelastic scattering.

Estimates of the production cross sections for four photons excited in the  $^{27}\text{Al}(n,p)^{27}\text{Mg}$  reaction are also included in the evaluation. These transi-

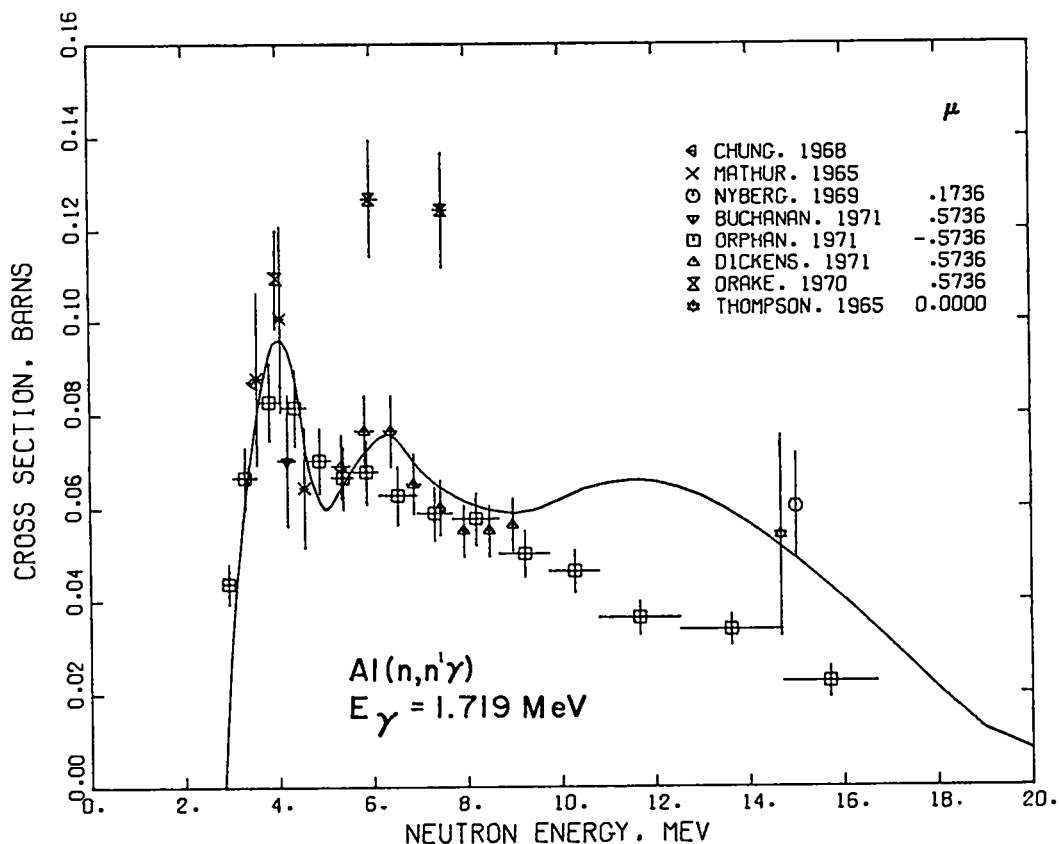


Fig. 43. Measured and evaluated  $^{27}\text{Al}(n,n'\gamma)$  cross section for the 1.719-MeV photon from the 2.732 + 1.013-MeV transition in  $^{27}\text{Al}$

TABLE IV  
GAMMA RAYS FROM THE  $^{27}\text{Al}(n,np)^{26}\text{Mg}$  REACTION

$E_\gamma$ (MeV)	$E_i$ (MeV)	$E_f$ (MeV)
4.313	4.313	0.
2.938	2.938	0.
2.522	{ 4.331 4.350 }	{ 1.809 1.809 }
2.132	3.941	0.
1.809	{ 1.809 3.585 }	{ 0. 1.809 }
1.40	{ 4.350 4.331 }	{ 2.938 2.938 }
1.129	2.938	1.809
1.003	{ 3.941 4.350 }	{ 2.938 3.585 }

tions are summarized in Table V. The results are based entirely on the Dickens measurements (D171), with a smooth extrapolation to 20 MeV.

TABLE V  
GAMMA RAYS FROM THE  $^{27}\text{Al}(n,p)^{27}\text{Mg}$  REACTION

$E_\gamma$ (MeV)	$E_i$ (MeV)	$E_f$ (MeV)
1.936	1.936	0.
1.692	1.692	0.
0.984	0.984	0.
0.952	1.936	0.984

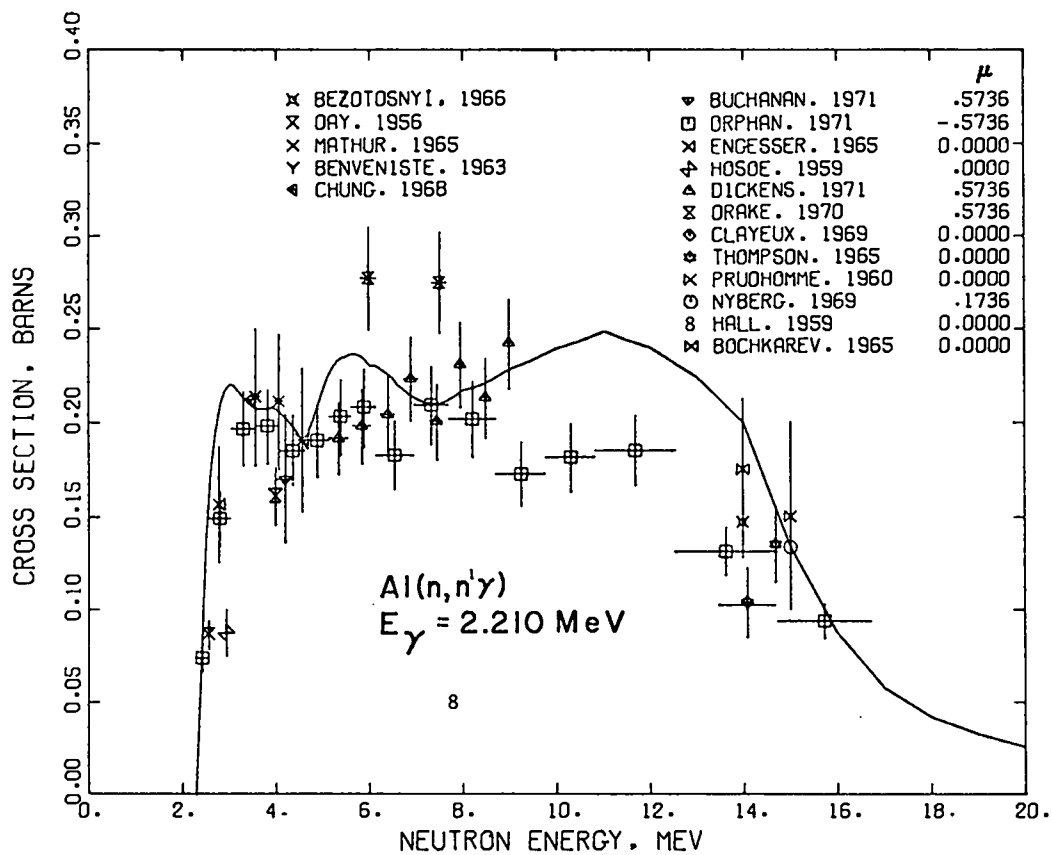


Fig. 44. Measured and evaluated  $^{27}Al(n,n'\gamma)$  cross section for the 2.210-MeV photon from the 2.210  $\rightarrow$  0-MeV transition in  $^{27}Al$ .

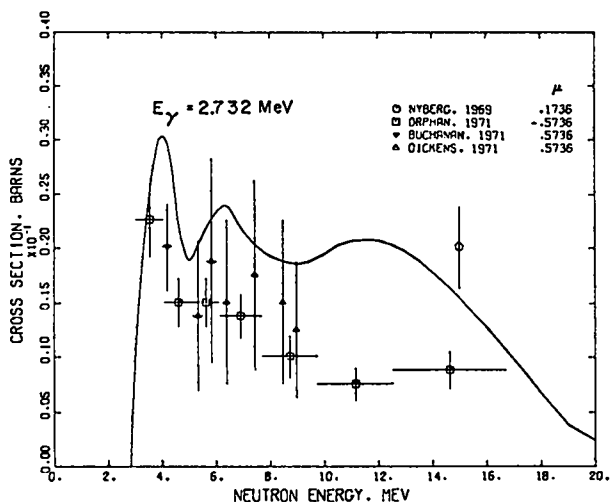


Fig. 45. Measured and evaluated  $^{27}Al(n,n'\gamma)$  cross section for the 2.732-MeV photon from the 2.732  $\rightarrow$  0-MeV transition in  $^{27}Al$ .

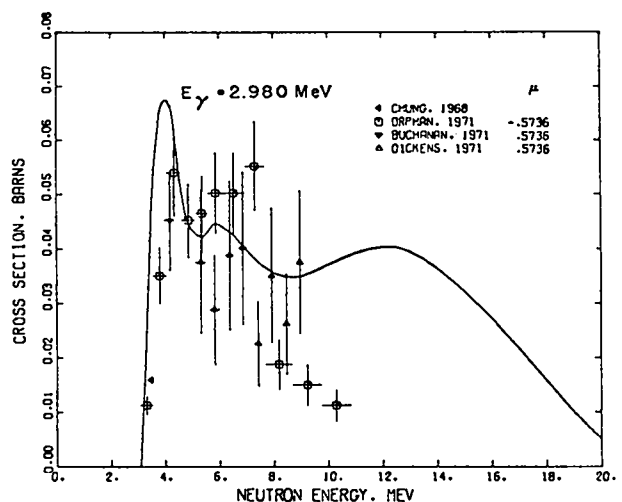


Fig. 46. Measured and evaluated  $^{27}Al(n,n'\gamma)$  cross section for the 2.980-MeV photon from the 2.980  $\rightarrow$  0-MeV transition in  $^{27}Al$ .

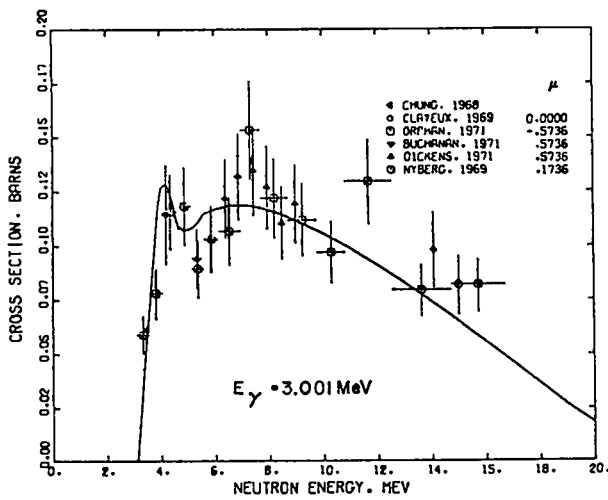


Fig. 47. Measured and evaluated  $^{27}\text{Al}(n,n'\gamma)$  cross section for the 3.001-MeV photon from the  $3.001 + 0$ -MeV transition in  $^{27}\text{Al}$ .

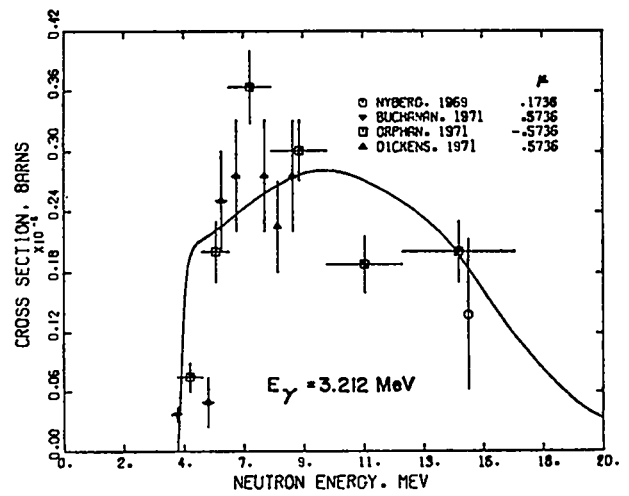


Fig. 49. Measured and evaluated  $^{27}\text{Al}(n,n'\gamma)$  cross section for the 3.212-MeV photon from the  $4.055 + 0.843$ -MeV transition in  $^{27}\text{Al}$ .

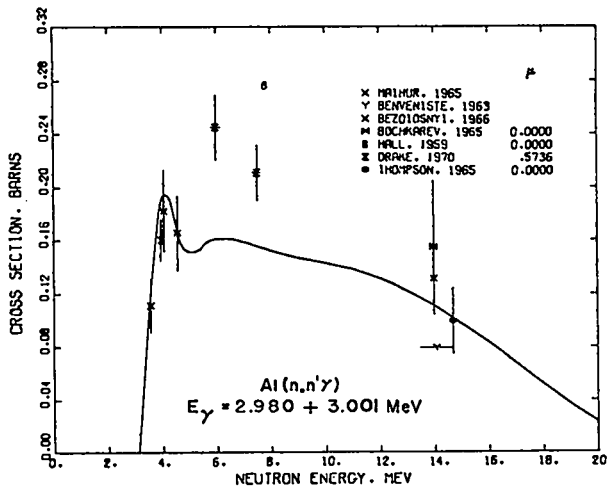


Fig. 48. Measured and evaluated  $^{27}\text{Al}(n,n'\gamma)$  cross section summed for the 2.980- and 3.001-MeV photons.

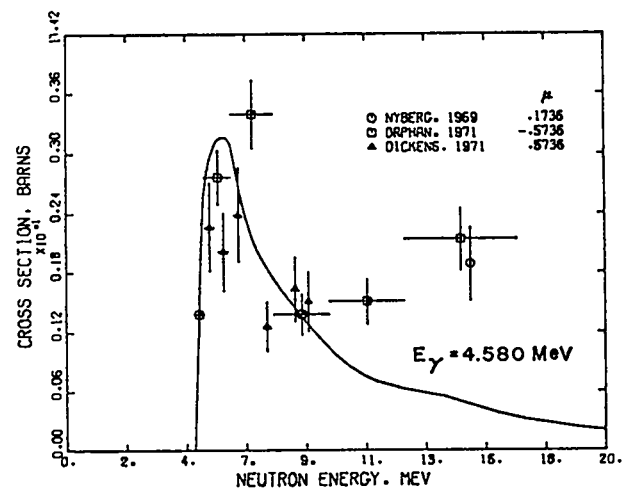


Fig. 50. Measured and evaluated  $^{27}\text{Al}(n,n'\gamma)$  cross section for the 4.580-MeV photon from the  $4.580 + 0$ -MeV transition in  $^{27}\text{Al}$ .

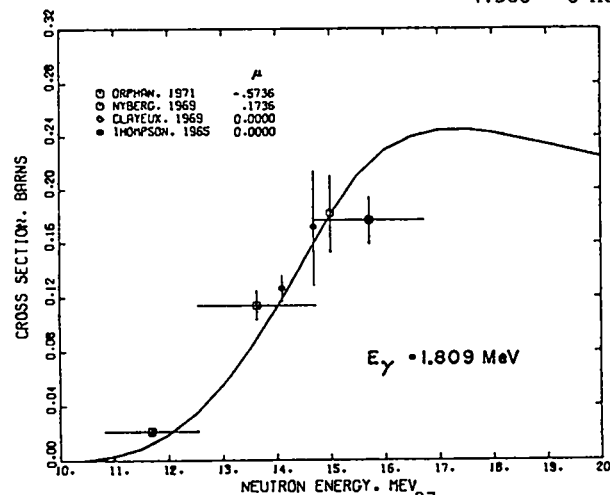


Fig. 51. Measured and evaluated  $^{27}\text{Al}(n,xy)$  cross section for the 1.809-MeV photon from the  $1.809 + 0$ -MeV transition in  $^{26}\text{Mg}$ .

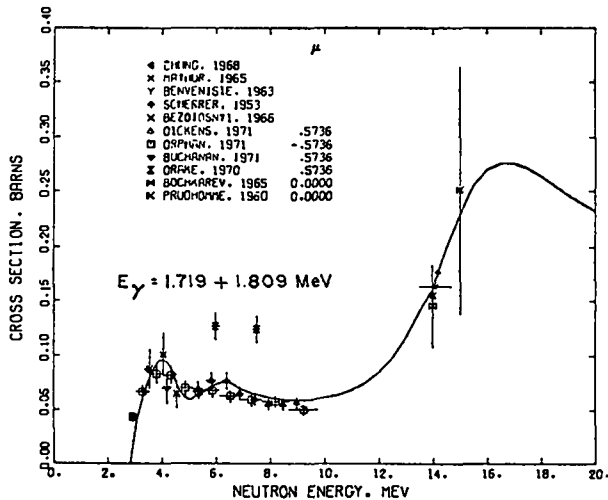


Fig. 52. Combined  $^{27}\text{Al}(n,xy)$  cross section for the 1.719- and 1.809-MeV photons, corresponding to the  $2.732 \rightarrow 1.013$ -MeV transition in  $^{27}\text{Al}$  and the  $1.809 \rightarrow 0$ -MeV transition in  $^{26}\text{Mg}$ , respectively.

### 3.2.2 Continuum Photons from $^{27}\text{Al}(n,xy)$ Reactions

At neutron energies above 5 MeV, an important component of the photon-production cross section results from transitions originating with levels in  $^{27}\text{Al}$  having  $E_x > 5$  MeV, either to other continuum levels or down to levels with  $E_x < 5$  MeV. To measure the cross sections for these unresolved photons, unfolding techniques are necessary that require high-quality data having good statistics and low background. Consequently, little information (Pe64, Dr70) of this nature existed until recently. For this evaluation, photon-energy spectra from continuum states formed in  $(n,n')$ ,  $(n,np)$ , and  $(n,2n)$  reactions were estimated from the statistical-theory calculations described in Sec. 3.2.1.

Comparisons are given in Figs. 53 and 54 between the evaluated photon spectra for all processes (including the resolved lines of Sec. 3.2.1) and the experimental results of Drake et al. (Dr70) at 7.5 MeV (Fig. 53) and the measurements of Orphan and Hoot (Or71) over two higher neutron-energy regions (Fig. 54).<sup>\*</sup> The Orphan results in Fig. 54 did not become available until after the evaluation was completed. The unresolved photons from the calculations appear at all photon energies in the figures; above  $E_\gamma \sim 5$  MeV, however, the evaluated curve is due en-

<sup>\*</sup>The comparisons given in Fig. 54 were provided by M. Fricke of GRT.

tirely to the calculated unresolved photon spectrum. The agreement between the evaluation and Drake's results shown in Fig. 53 is poor, particularly because unresolved photons with  $E_\gamma > 4.5$  MeV were not observed in the measurements. The evaluated results are in better agreement with Orphan's measurements in Fig. 54, particularly for higher photon energies.

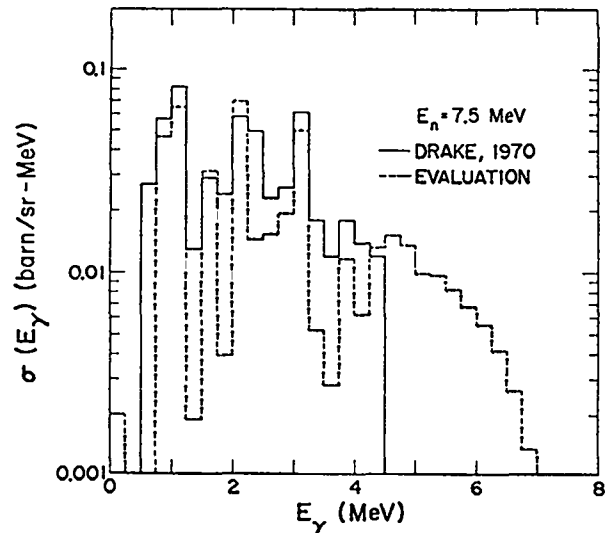


Fig. 53. Measured and evaluated photon energy spectra from all reactions at  $E_n = 7.5$  MeV.

In Fig. 55 we compare the total gamma-ray production cross section measured by Orphan and Hoot (Or71) to the evaluated curve. The data in Fig. 55 include all photons from all reactions. The evaluated curve appears to be somewhat low in the 5- to 9-MeV region, although it is generally within 20% of the measured values. The dip in the curve above 13 MeV results mainly from the onset of the  $(n,2n)$  reaction.

## 4. NEUTRON ENERGY DISTRIBUTIONS

The  $(n,n')$ ,  $(n,np)$ , and  $(n,n\alpha)$  reactions were treated as  $(n,n')$  reactions to levels or groups of levels (Secs. 2.4 and 2.5) that decay by emission of photons, protons, or alpha particles. The energy distributions of secondary neutrons from these processes are implicit in this representation, and no further information is required.

The threshold for the  $(n,2n)$  reaction is 13.55 MeV, and there are no experimental data available for the energy distributions of secondary neutrons from that reaction. Therefore, the neutron spectra

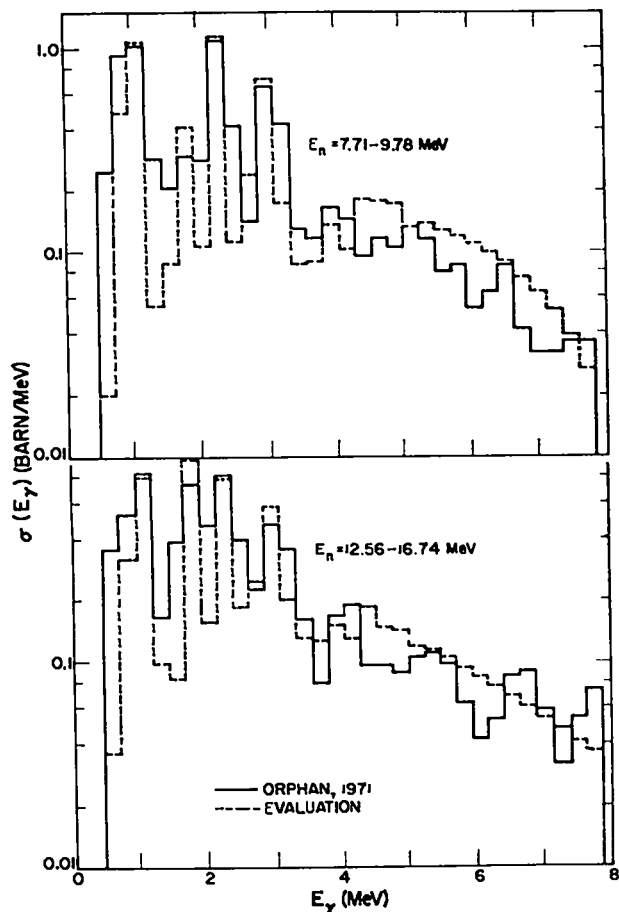


Fig. 54. Measured and evaluated photon energy spectra from all reactions averaged over the neutron energy regions 7.71-9.78 MeV and 12.56-16.74 MeV.

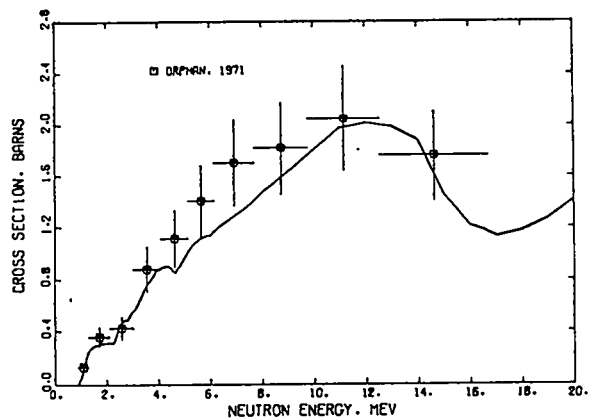
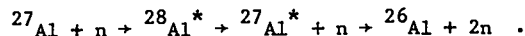


Fig. 55. Measured and evaluated total photon-production cross section from all  $^{27}\text{Al}(n,\gamma)$  reactions.

from the  $(n,2n)$  reaction were estimated from the statistical-theory calculations described in Sec. 3.2.1. In the calculations, the  $(n,2n)$  reaction was assumed to proceed in the sequence



The decay of  $^{28}\text{Al}^*$  and  $^{27}\text{Al}^*$  by neutron emission was assumed to follow Eq. (3), with the additional assumption of equal branching for proton and neutron emission from  $^{27}\text{Al}^*$ . We used Eq. (5) to express the level density. The nuclear temperature defined by Eq. (2) was used for  $^{28}\text{Al}^*$  and  $^{27}\text{Al}^*$ , with an appropriate adjustment made for the  $(n,2n)$  Q-value in the latter case.

## 5. ANGULAR DISTRIBUTIONS

### 5.1. Elastic Neutron Angular Distributions

The angular distributions of neutrons from elastic scattering were taken as isotropic below 100 keV, and no attempt was made to include anisotropy near the large resonances. From 0.1 to 8 MeV, Legendre coefficients were derived from all available data sets that were complete enough to fit (mainly La57, Ch66, To62, Ts61, Ki70, and Be58). The coefficients used for the evaluation were obtained by drawing smooth curves through plots of the fitted values, thus completely averaging over the resonance structure. The resulting coefficients for  $l > 0$  were increased empirically by up to 20% between 2.5 and 5 MeV to avoid violating Wick's limit (Wi49). Representative comparisons between the measured and evaluated angular distributions at neutron energies below 8 MeV are given in Figs. 56-58.

To obtain the distributions at higher energies, optical-model calculations, using the Agee-Rosen parameters (Ag66), were compared to the cluster of measurements between 14 and 15 MeV, and to the 24-MeV measurement of Stuart et al. (St62). Without attempting to refine the parameters, we altered the calculated angular distributions empirically to improve agreement with experiment, and new Legendre coefficients were derived from the adjusted distributions. A smooth interpolation from 8 to 14 MeV was then made. The Legendre coefficients that resulted lead to non-negative distributions at all neutron energies, and do not violate Wick's lower limit (Wi49) for the  $0^\circ$  cross section. The result-

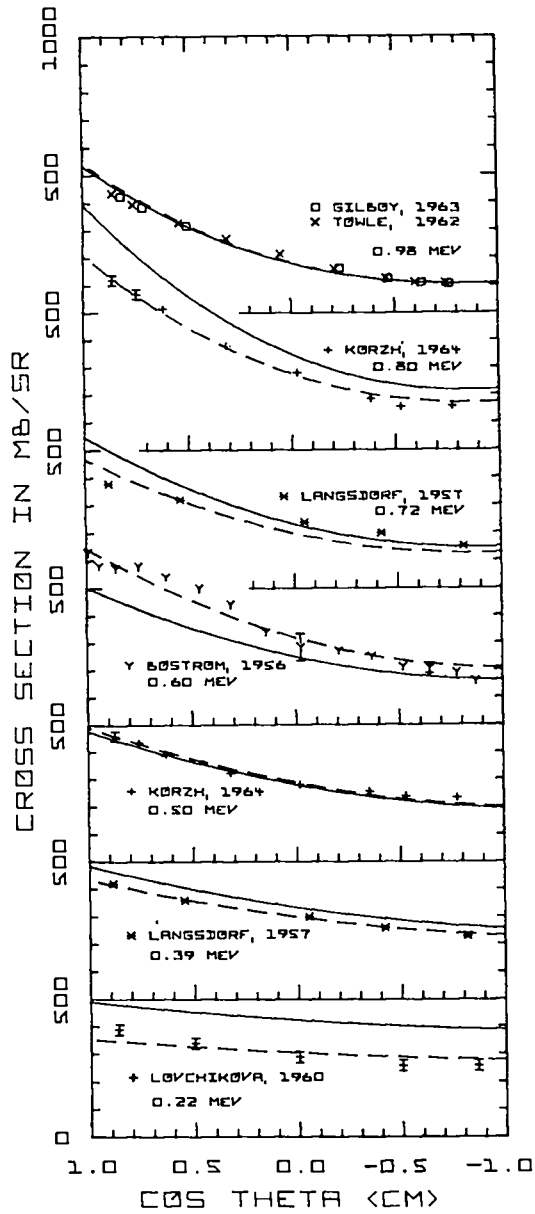


Fig. 56. Measured and evaluated angular distributions for elastic scattering from 0.22 to 0.98 MeV. The dashed curves represent the evaluated shapes normalized to the measurements; the solid curve gives the same shapes normalized to the evaluated elastic cross sections.

ing differential cross sections are compared to the measurements between 8 and 15 MeV in Fig. 59.

### 5.2. Nonelastic Neutron Angular Distributions

The angular distributions of secondary neutrons from all  $(n,n')$  reactions, including  $(n,np)$  and  $(n,n\alpha)$ , are assumed to be isotropic in the center-of-mass system. The extensive comparisons given by

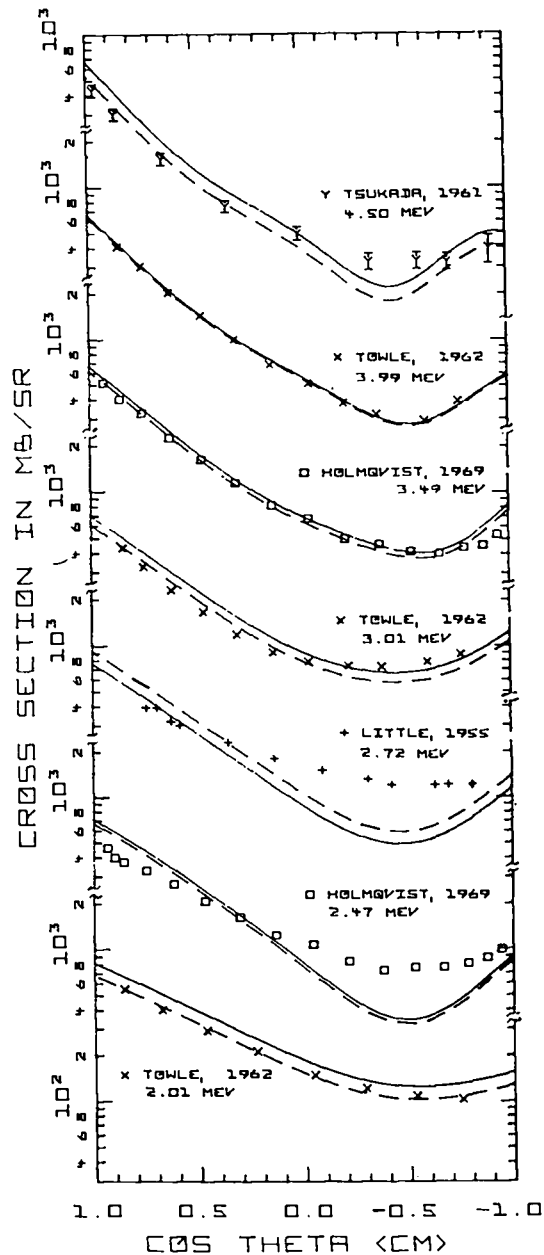


Fig. 57. Measured and evaluated angular distributions for elastic scattering from 2.01 to 4.50 MeV. See caption to Fig. 56 for details.

Kinney and Perey (Ki70) of their inelastic angular distribution measurements with the results of other authors indicate that isotropy is usually a reasonable assumption. There are examples, of course, where isotropy does not hold but the deviations are generally not too severe.

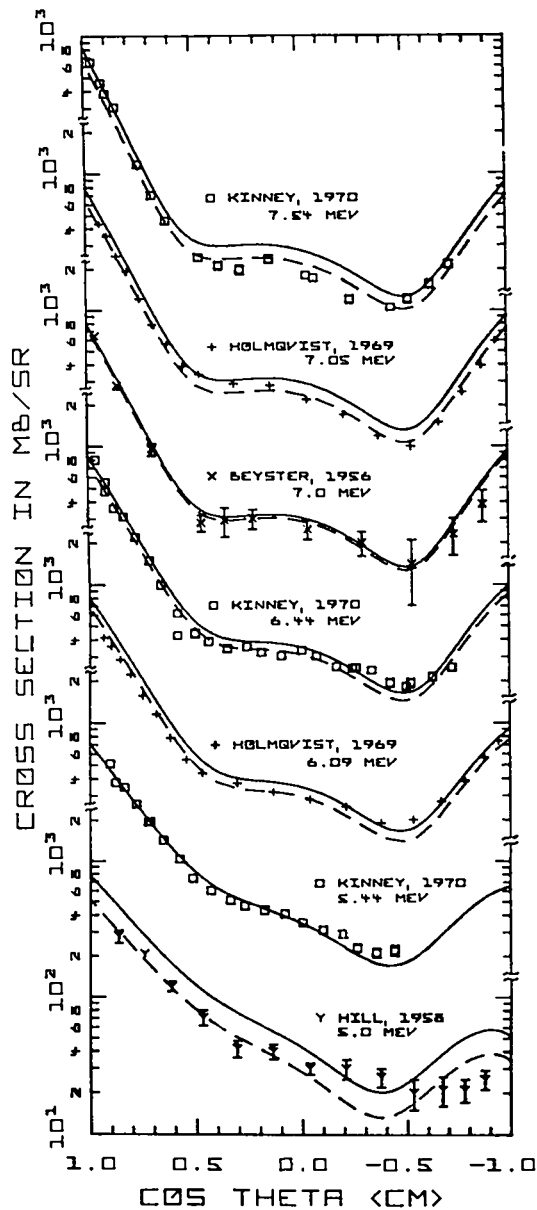


Fig. 58. Measured and evaluated angular distributions for elastic scattering from 5.0 to 7.54 MeV. See caption to Fig. 56 for details.

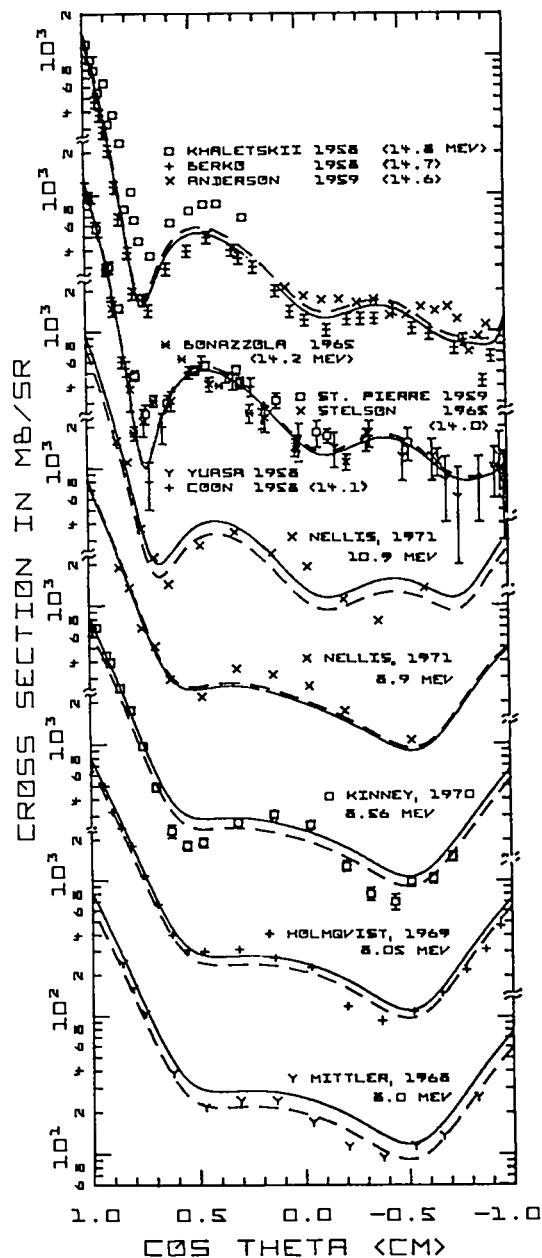


Fig. 59. Measured and evaluated angular distributions for elastic scattering from 8.0 to 14.8 MeV. See caption to Fig. 56 for details.

No data are available for the angular distributions of neutrons from the  $(n,2n)$  reaction. For this evaluation laboratory angular distributions were provided for the  $(n,2n)$  energy spectra discussed in Sec. 4. These distributions were obtained by assuming isotropic emission of a dineutron in the center-of-mass system and performing a two-body

transformation to the laboratory system. At each incident neutron energy, average Q-values that were obtained from the energy spectra were used in the calculations.

### 5.3. Secondary Photon Angular Distributions

All secondary photons from both  $(n,\gamma)$  and  $(n,x\gamma)$  reactions are assumed in the evaluation to be iso-

tropic in the laboratory system. For the (n, $\gamma$ ) reaction, no data are available on the angular distributions, but the assumption of isotropy would certainly be valid at low neutron energies where s-wave capture dominates and where the cross section is largest.

The assumption of isotropy for  $^{27}\text{Al}(n,x\gamma)$  reactions is generally supported by Dickens' measurements (Di71) at 55, 75, and 90°. There are exceptions, of course. The more complete angular-distribution measurements by Chung et al. (Ch68) at  $E_n = 3.5$  MeV indicate significant anisotropies for the 2.210-MeV photon [ $\sigma(0^\circ)/\sigma(90^\circ) \sim 1.2$ ] and for the 3.001-MeV photon [ $\sigma(0^\circ)/\sigma(90^\circ) \sim 1.4$ ], although less pronounced effects were observed for these photons by Mathur et al. (Ma65) between 3.57 and 4.57 MeV. The other photons observed in these two measurements (Ch68, Ma65) are nearly isotropic.

## 6. DISCUSSION

There are several areas in the present evaluation where improvements can be made. A better treatment of the resonance structure in the elastic cross sections and angular distributions in the keV region would be useful, and greater application of model codes should improve the elastic results at higher

neutron energies. A more thorough study of the inelastic cross-section measurements would improve these data, particularly if greater use were made of theoretical calculations. Further, an extensive new measurement of neutron energy spectra as a function of angle has been made by Kammerdiener (Ka72) for 14-MeV incident neutrons, and inclusion of these data should improve the inelastic results at that energy. There are preliminary indications (Mu72) from calculations of time-dependent neutron spectra emerging from aluminum spheres pulsed with 14-MeV neutrons (Ha70) that the inelastic data need improvement at 14-MeV. Better estimates for some of the charged-particle emission cross sections can be made with recently improved model codes such as COMNUC (Du71). The capture gamma-ray energy spectrum can be upgraded on the basis of existing measurements, and the new extensive results by Orphan and Hoot (Or71) should improve the (n, $x\gamma$ ) cross sections and secondary-photon spectra. Finally, improvements are possible in the inelastic-neutron and secondary-photon angular distributions on the basis of existing measurements and nuclear theory.

A summary of estimated uncertainties in the various cross sections is included in Table VI. These errors represent order-of-magnitude averages

TABLE VI  
ESTIMATED ERRORS IN THE EVALUATED CROSS SECTIONS OF  $^{27}\text{Al}$

Cross Section	ENDF/B Designation	Neutron Energy (MeV)									
		Thermal	0.01	0.1	1	3	5	8	11	14	20
Total	MF=3,MT=1	± 5%	± 5%	± 4%	± 2%	± 2%	± 2%	± 2%	± 2%	± 2%	± 2%
Elastic	MF=3,MT=2	5%	5%	4%	3%	5%	8%	12%	20%	15%	20%
Nonelastic	MF=3,MT=3	4%	20%	20%	30%	15%	10%	10%	15%	10%	20%
Total (n,n')	MF=3,MT=4	-	-	-	30%	15%	10%	10%	15%	15%	30%
(n,2n)	MF=3,MT=16	-	-	-	-	-	-	-	-	50%	50%
Discrete (n,n') $E_x < 5$ MeV	MF=3,MT=51-63	-	-	-	30%	15%	15%	20%	25%	30%	50%
Discrete (n,n') $E_x > 5$ MeV	MF=3,MT=64-90	-	-	-	-	-	-	50%	50%	50%	50%
(n, $\gamma$ )	MF=3,MT=102	4%	20%	20%	20%	20%	20%	50%	50%	20%	x2
(n,p)	MF=3,MT=103	-	-	-	-	30%	20%	20%	20%	15%	20%
(n,d)	MF=3,MT=104	-	-	-	-	-	-	-	50%	50%	50%
(n,t)	MF=3,MT=105	-	-	-	-	-	-	-	-	-	50%
(n, $\alpha$ )	MF=3,MT=107	-	-	-	-	-	-	15%	15%	10%	10%
Total (n, $x\gamma$ )	MF=13, Sum of MT=4,28,103	-	-	-	30%	15%	15%	20%	20%	20%	40%
Individual (n, $x\gamma$ ) Lines	MF=13 MT=4,28,103	-	-	-	30%	15%	15%	20%	25%	30%	50%

over broad energy groups and are not expected to hold true in detail. In addition, we made no attempt to estimate the errors due to unknown structure in the cross sections. The accuracy of the elastic angular distributions is expected to be generally  $\pm 15\%$ , although larger errors will certainly occur in regions of structure.

#### ACKNOWLEDGMENTS

We wish to thank D. M. McClellan, C. I. Baxman, and N. Whittemore for their help with the many clerical tasks required for this work and E. T. Jurney for his many useful comments. Finally, we gratefully acknowledge the many authors who provided us with their experimental results in advance of publication.

#### REFERENCES

- Ag66 F. P. Agee and L. Rosen, "Calculations of Neutron Cross Sections Using A Local Optical Potential with Average Parameters," Los Alamos Scientific Laboratory report LA-3538-MS (1966).
- Al57 D. L. Allan, "Protons from the Interaction of 14-MeV Neutrons with Medium Weight Nuclei," Proc. Phys. Soc. (London) A70, 195 (1957).
- Al61 D. L. Allan, "An Experimental Test of the Statistical Theory of Nuclear Reactions," Nucl. Phys. 24, 274 (1961).
- An59 J. D. Anderson, C. C. Gardner, J. W. McClure, M. P. Nakada, and C. Wong, "Back-Angle Elastic Scattering of 14.6-MeV Neutrons from Aluminum, Copper, and Zirconium," Phys. Rev. 115, 1010 (1959).
- Ar64 P. M. Aron, S. S. Bugorkov, K. A. Petrzhak, and A. V. Sorokina, "Radio-Chemical Determination of the  $Al^{27}(n,\alpha)Na^{24}$  Reaction Cross Section for a Neutron Energy of 14.6 MeV," At. Energiya (trans.) 16, 450 (1964).
- Ar65 B. H. Armitage, J. H. Montague, N. Nath, A. K. M. Siddiq, and D. C. Stuegia, "Production Cross Sections of Gamma Rays by Inelastic Neutron Scattering from  $^{27}Al$ ," Proceedings of the International Conference on the Study of Nuclear Structure with Neutrons, Antwerp, 1965 (North Holland Publishing Co., Amsterdam, 1966) p. 503.
- Ar67 A. P. Arya, D. L. Campbell, and R. D. Wilson, " $\gamma$  Yield from 14.3-MeV Neutron Inelastic Scattering and Comparison with Quadrupole Transitions," Bull. Am. Phys. Soc. 12, 124 (1967).
- Ba58 W. P. Ball, M. MacGregor, and R. Booth, "Neutron Nonelastic Cross Sections from 7 to 14 MeV," Phys. Rev. 110, 1392 (1958).
- Ba58a G. A. Bartholomew and L. A. Higgs, "Compilation of Thermal-Neutron Capture Gamma Rays," Atomic Energy of Canada Ltd. report AECL-669 (1958).
- Ba61 B. P. Bayhurst and R. J. Prestwood, "(n,2n), (n,p), and (n, $\alpha$ ) Excitation Functions of Several Nuclei from 7.0 to 19.8 MeV," Los Alamos Scientific Laboratory report LA-2493 (1961); R. J. Prestwood and B. P. Bayhurst, "(n,2n) Excitation Functions of Several Nuclei from 12.0 to 19.8 MeV," Phys. Rev. 121, 1438 (1961).
- Ba65 R. Bass, P. Haug, K. Krüger, and B. Staginnus, "Fast Neutron Excitation Functions by Activation Techniques," European-American Nuclear Data Committee report EANDC(E)-66U (1966) p. 64, and private communication from R. Bass (1971).
- Ba67 G. A. Bartholomew, A. Doveika, K. M. Eastwood, S. Monaro, L. V. Groshev, A. M. Demidov, V. I. Pelekhov, and L. L. Sokolovskii, "Compendium of Thermal-Neutron-Capture  $\gamma$ -Ray Measurements, Part 1,  $Z \leq 46$ ," Nucl. Data A3, 367 (1967).
- Ba69 R. C. Barrall, M. Silbergeld, and D. G. Gardner, "Cross Sections of some Reactions of Al, S, Mn, Fe, Ni, In, and I with 14.8-MeV Neutrons," Nucl. Phys. A138, 387 (1969).
- Be55 J. R. Beyster, R. L. Henkel, R. A. Nobles, and J. M. Kister, "Inelastic Collision Cross Sections at 1.0-, 4.0- and 4.5-MeV Neutron Energies," Phys. Rev. 98, 1216 (1955).
- Be56 J. R. Beyster, M. Walt, and E. W. Salmi, "Interaction of 1.0-, 1.77-, 2.5-, 3.25-, and 7.0-MeV Neutrons with Nuclei," Phys. Rev. 104, 1319 (1956).
- Be58 S. Berko, W. D. Whitehead, and B. C. Groseclose, "Angular Distribution of Elastically Scattered 14.7-MeV Neutrons," Nucl. Phys. 6, 210 (1958).
- Be63 J. Benveniste, N. Chazan, and A. Mitchell, "Spectra of Continuum Gamma Rays Resulting from 14-MeV Neutron Interactions with Several Elements," University of California Radiation Laboratory report UCRL-7440 (UCID-4619) (1963).
- Be66 V. M. Bezotosnyi, V. G. Vershinin, L. M. Surov, and M. S. Shvetsov, "Cross Sections for the Production of Gamma Quanta in Inelastic Interaction Between 14-MeV Neutrons and C, O, Al, Fe, and Pb Nuclei," Sov. J. Nucl. Phys. 3, 632 (1966).
- B168 R. C. Block, private communication to R. J. Howerton (1968).
- Bo56 N. A. Bostrom and I. L. Morgan, private communication to Sigma Center, Brookhaven National Laboratory (1956).
- Bo61 M. Bormann, S. Cierjacks, R. Langkau, H. Neuert, and H. Pollehn, "Mesure de quelques Sections Efficaces (n, $\alpha$ ) dans l'Intervalle des Energies des Neutrons 12 a 19.6 MeV," J. Phys. Radium 22, 602 (1961).
- Bo64 G. C. Bonazzola, P. Brovotto, E. Chlavassa, R. Spinoglio, and A. Pasquarelli, "The Measurement by Activation of Cross Sections for 14.7-MeV Neutrons," Nucl. Phys. 51, 337 (1964).

- Bo65 V. N. Bochkarev and V. V. Nefedov, " $\gamma$  Radiation from the Inelastic Interaction of 14-MeV Neutrons with Magnesium, Aluminum, and Sulfur Nuclei," *Sov. J. Nucl. Phys.* 1, 574 (1965).
- Bo65a G. C. Bonazzola, E. Chiayassa, and T. Bressani, "Excited-Core Model in  $Al^{27}$  and Inelastic Scattering of 14.2-MeV Neutrons," *Phys. Rev.* 140, B835 (1965).
- Bo65b M. Bormann, E. Fretwurst, P. Schehka, G. Wrege, H. Büttner, A. Lindner, and H. Meldner, "Some Excitation Functions of Neutron-Induced Reactions in the Energy Range 12.6-19.6 MeV," *Nucl. Phys.* 63, 438 (1965).
- Br64 D. J. Bredin, "Scattering and Polarization of Neutrons from Al, Si, Fe, and Co at 2 MeV," *Phys. Rev.* 135, B412 (1964).
- Bu63 J. P. Butler and D. C. Santry, "Excitation Curves for the Reactions  $Al^{27}(n,\alpha)Na^{24}$  and  $Mg^{24}(n,p)Na^{24}$ ," *Can. J. Phys.* 41, 372 (1963).
- Bu71 P. S. Buchanan, D. O. Nellis, and W. E. Tucker, "A Compilation of Cross Sections and Angular Distributions of Gamma Rays Produced by Neutron Bombardment of Various Nuclei," Texas Nuclear Corporation report ORO-2791-32 (1971).
- Ca62 G. Calvi, R. Potenza, R. Ricamo, and D. Vinciguerra, "Neutron Reactions in Al from 2.5 to 5 MeV," *Nucl. Phys.* 39, 621 (1962).
- Ca67 A. D. Carlson and H. H. Barschall, "Fluctuations in Neutron Total Cross Sections," *Phys. Rev.* 158, 1142 (1967).
- Ch63 G. P. Chursin, V. Yu. Gonchar, I. I. Zalyubovskii, and A. P. Klyucharev, "Cross Sections for (n,p) Reactions on Tin Isotopes for 14.5-MeV Neutrons," *Sov. Phys. -JETP* 17, 321 (1963).
- Ch66 J. P. Chien and A. B. Smith, "Fast Neutron Scattering from Beryllium, Sodium, and Aluminum," *Nucl. Sci. Eng.* 26, 500 (1966).
- Ch67 A. Chatterjee and A. M. Ghose, "Nonelastic Cross Sections of Nuclei for 14.8-MeV Neutrons," *Phys. Rev.* 161, 1181 (1967).
- Ch68 K. C. Chung, D. E. Velkley, J. D. Brandenberger, and M. T. McEllistrem, " $^{27}Al(n,n'\gamma)$  Reactions and the 3002-keV Level," *Nucl. Phys.* A115, 476 (1968).
- Ci68 S. Cierjacks, P. Forti, D. Kopsch, L. Kropp, J. Nebe, and H. Unseld, "High Resolution Total Neutron Cross Sections between 0.5 and 30 MeV," Kernforschungszentrum Karlsruhe report KFK-1000, Karlsruhe, Germany (1968).
- Ci69 G. Clayeux and G. Grenier, "Spectres de Renvoi des Gammas Produits par des Neutrons de 14.1 MeV," Centre d'Etudes de Limeil report CEA-R-3807, Limeil, France (1969).
- Co58 J. H. Coon, R. W. Davis, H. E. Felthouser, and D. B. Nicodemus, "Scattering of 14.5-MeV Neutrons by Complex Nuclei," *Phys. Rev.* 111, 250 (1958), and private communication to R. J. Howerton (1959).
- Cs63 J. Csikai, B. Gyarmati, and I. Hunyadi, "Activation Cross-Sections for  $Na^{23}$  and  $Al^{27}$  with 14-MeV Neutrons," *Nucl. Phys.* 46, 141 (1963).
- Cs67 J. Csikai, G. Petö, M. Buczkó, Z. Miligy, and N. A. Elssa, "Radiative Capture Cross Sections for 14.7-MeV Neutrons," *Nucl. Phys.* A95, 229 (1967).
- Cu68 P. Cuzzocrea, E. Perillo, and S. Notarrigo, "Some Excitation Functions of Neutron-Induced Reactions around 14 MeV," *Nuovo Cimento* B54, 53 (1968).
- Da56 R. B. Day, "Gamma Rays from Neutron Inelastic Scattering," *Phys. Rev.* 102, 767 (1956).
- De60 M. J. DePraz, G. Legros, and M. R. Salin, "Mesure des Sections Efficaces de quelques Reactions (n,p), (n, $\alpha$ ), (n,2n)," *J. Phys. Radium* 21, 377 (1960).
- De61 Yu. G. Degtyarev and V. G. Nadtochi, "Measurement of the Cross Sections for Inelastic Interaction of Neutrons with an Energy of 13 to 20 MeV Using Certain Isotopes," *Sov. J. At. Energy* 11, 1043 (1961).
- De65 Yu. G. Degtyarev, "Non-Elastic Interaction Cross Sections of Neutrons with  $^7Li$ ,  $^{12}C$ ,  $^{14}N$ ,  $^{27}Al$ ,  $^{56}Fe$ , Cu, Pb,  $^{235}U$ ,  $^{238}U$ , and  $^{239}Pu$ ," *J. Nucl. Energy* 20, 818 (1965).
- Di71 J. K. Dickens, " $Al(n,xy)$  Reactions for  $5.3 \leq E_n \leq 9.0$  MeV," Oak Ridge National Laboratory report ORNL-TM-3284 (1971).
- Dr63 J. E. Draper and C. O. Bostrom, "Transition Intensities from Thermal (n, $\gamma$ ) in Be, Al, Cl, Sc, and Ti," *Nucl. Phys.* 47, 108 (1963).
- Dr70 D. M. Drake, J. C. Hopkins, C. S. Young, and H. Condé, "Gamma-Ray-Production Cross Sections for Fast-Neutron Interactions with Several Elements," *Nucl. Sci. Eng.* 40, 294 (1970).
- Du71 C. L. Dunford, private communication (1971); see also C. L. Dunford, "A Unified Model for Analysis of Compound Nucleus Reactions," *Atomics International* report AI-AEC-12931 (1970).
- E168 R. V. Elliott, T. R. Ophel, and R. H. Spear, "Branching Ratios of  $^{27}Al$  Bound States," *Nucl. Phys.* A115, 673 (1968).
- En65 F. C. Engesser and W. E. Thompson, "Gamma Rays from (n,n' $\gamma$ ) Interactions of 2.8-MeV Neutrons with Magnesium, Aluminum, Silicon, Titanium, and Iron," Naval Radiological Defense Laboratory report USNRDL-TR-916 (1965).
- En67 P. M. Endt and C. van der Leun, "Energy Levels of  $Z = 11-21$  Nuclei (IV)," *Nucl. Phys.* A105, 1 (1967).
- Fe67 J. M. Ferguson and J. C. Albergotti, "Structure in the Total  $^{24}Mg(n,p)$ ,  $^{27}Al(n,p)$ , and  $^{27}Al(n,\alpha)$  Cross Sections from 12 to 15 MeV," *Nucl. Phys.* A98, 65 (1967).

- F156 N. N. Flerov and V. M. Talyzin, "Cross Section for Inelastic Interactions of 14.5-MeV Neutrons with Various Elements," *At. Energiya* 1, 155 (1956).
- Fo52 S. G. Forbes, "Activation Cross Sections for 14-MeV Neutrons," *Phys. Rev.* 88, 1309 (1952).
- Fo71 D. G. Foster, Jr. and D. W. Glasgow, "Neutron Total Cross Sections, 2.5-15 MeV. I. Experimental," *Phys. Rev. C* 3, 576 (1971).
- Ga62 F. Gabbard and B. D. Kern, "Cross Sections for Charged-Particle Reactions Induced in Medium Weight Nuclei by Neutrons in the Energy Range 12-18 MeV," *Phys. Rev.* 128, 1276 (1962).
- Ga65 J. B. Garg, J. Rainwater, J. S. Petersen, and W. W. Havens, Jr., private communication to R. J. Howerton (1965); see also U. N. Singh, J. B. Garg, J. Rainwater, W. W. Havens, Jr., and S. Wynchank, "High Resolution Spectroscopy in the keV Region-F, Al," *Bull. Am. Phys. Soc.* 16, 495 (1971).
- Gl61 J. H. Gibbons, R. L. Macklin, P. D. Miller, and J. H. Neiler, "Average Radiative Capture Cross Sections for 7- to 170-keV Neutrons," *Phys. Rev.* 122, 182 (1961).
- Gl63 W. B. Gilboy and J. H. Towle, "Elastic Scattering of 1 MeV Neutrons," *Nucl. Phys.* 42, 86 (1963).
- Gl61 R. N. Glover and E. Weigold, "Protons and Deuterons from  $Al^{27}$  Bombarded by 14.8 MeV Neutrons," *Nucl. Phys.* 24, 630 (1961).
- G172 D. W. Glasgow, private communication (1972).
- Go71 D. T. Goldman, P. Aline, R. Sher, and J. R. Stehn, unpublished evaluation (1971).
- Gr53 E. R. Graves and L. Rosen, "Distribution in Energy of the Neutrons from the Interaction of 14-MeV Neutrons with some Elements," *Phys. Rev.* 89, 343 (1953).
- Gr55 E. R. Graves and R. W. Davis, "Cross Sections for Nonelastic Interactions of 14-MeV Neutrons with Various Elements," *Phys. Rev.* 97, 1205 (1955).
- Gr58 J. A. Grundl, R. L. Henkel, and B. L. Perkins, " $p^{31}(n,p)Si^{31}$  and  $Al^{27}(n,\alpha)Na^{24}$  Cross Sections," *Phys. Rev.* 109, 425 (1958).
- Gr59 L. V. Groshev, A. M. Demidov, V. N. Lutsenko, and V. I. Pelikhov, Atlas of  $\gamma$ -Ray Spectra from Radiative Capture of Thermal Neutrons (Pergamon Press, New York, 1959).
- Gr65 R. C. Greenwood and J. H. Reed, "Prompt Gamma Rays from Radiative Capture of Thermal Neutrons," IIT Research Institute report IITRI-1193-53, (1965), p. 120.
- Gr67 J. A. Grundl, "A Study of Fission-Neutron Spectra with High-Energy Activation Detectors-Part 1. Detector Development and Excitation Measurements," *Nucl. Sci. Eng.* 30, 39 (1967).
- Ha59 H. E. Hall and T. W. Bonner, "Inelastic Scattering of Fast Neutrons by  $N^{14}$  and  $Al^{27}$ ," United States Atomic Energy Commission report WASH-1021 (1959), p. 52.
- Ha62 F. L. Hassler and R. A. Peck, Jr., "Neutron-Induced Reactions in Third and Fourth Shell Nuclei," *Phys. Rev.* 125, 1011 (1962).
- Ha68 S. S. Hasan, A. K. Chaubey, and M. L. Sehgal, "Study of the Average Level Spacing from Neutron-Capture Cross Section," *Nuovo Cimento* 58B, 402 (1968).
- Ha68a O. Häusser, D. Pelte, and J. F. Sharpey-Schafer, "The 4509-keV Level in  $^{27}Al$ ," *Can. J. Phys.* 46, 1145 (1968).
- Ha69 R. Hardell, S. O. Idetjärn, and H. Ahlgren, "Thermal-Neutron Capture Gamma Rays from the  $^{27}Al(n,\gamma)^{28}Al$  Reaction," *Nucl. Phys.* A126, 392 (1969).
- Ha70 L. F. Hansen, J. D. Anderson, E. Goldberg, J. Kammerdiener, E. Plechaty, and C. Wong, "Predictions for Neutron Transport in Air, Based on Integral Measurements in Nitrogen and Oxygen at 14 MeV," *Nucl. Sci. Eng.* 40, 262 (1970); L. F. Hansen, J. D. Anderson, J. L. Kammerdiener, and C. Wong, "Sensitivity of Monte Carlo Calculations to the Neutron Cross Sections for Neutron Transport in Nitrogen and in Air," Lawrence Livermore Laboratory report UCRL-51031 (1971).
- He50 R. L. Henkel and H. H. Barschall, "Capture Cross Sections for Fast Neutrons," *Phys. Rev.* 80, 145 (1950).
- He53 R. L. Henkel, private communication to Sigma Center, Brookhaven National Laboratory (1953).
- He54 R. L. Henkel, private communication to Sigma Center, Brookhaven National Laboratory (1954).
- He66 J. D. Hemingway, R. H. James, E. B. M. Martin, and G. R. Martin, "The Determination of the Cross Sections for the Reactions  $^{27}Al(n,\alpha)$  and  $^{56}Fe(n,p)$  for 14 MeV Neutrons by an Absolute Method," *Proc. Roy. Soc. (London)* A292, 180 (1966).
- Hi49 C. T. Hibdon and C. O. Muehlhause, "Neutron Cross Sections at 115 eV and 300 eV-I," *Phys. Rev.* 76, 100 (1949).
- Hi58 R. W. Hill, "Angular Distributions of Elastic Scattering of 5-MeV Neutrons," *Phys. Rev.* 109, 2105 (1958).
- Hi59 C. T. Hibdon, "Distribution of the Angular Momenta, Level Spacings, and Neutron Widths of  $Al^{28}$ ," *Phys. Rev.* 114, 179 (1959).
- H164 C. T. Hibdon, private communication to Sigma Center, Brookhaven National Laboratory (1964).
- Ho59 M. Hosoe and S. Suzaki, "Gamma Rays from Neutron Inelastic Scattering of Magnesium, Aluminum, Iron and Bismuth," *J. Phys. Soc. Japan* 14, 699 (1959).

- Ho69 B. Holmqvist and T. Wiedling, "Neutron Elastic Scattering Cross Sections; Experimental Data and Optical Model Cross Section Calculations," Aktiebolaget Atomenergi report AE-366, Studsvik, Sweden (1969).
- Hu59 O. M. Hudson, Jr. and I. L. Morgan, "Fast Neutron Activation of Al," Bull. Am. Phys. Soc. 4, 97 (1959).
- Hu69 F. C. P. Huang and T. R. Ophel, "Resonances of the  $^{26}\text{Mg}(p,\gamma)$  Reaction between 660 and 1000 keV," Nucl. Phys. A135, 647 (1969).
- Hu70 L. Husain, A. Bari, and P. K. Kuroda, "Neutron Activation Cross Sections at 14.8 MeV for Rubidium, Strontium, Zirconium, and Niobium," Phys. Rev. C 1, 1233 (1970).
- Im60 W. L. Imhof, private communication to Sigma Center, Brookhaven National Laboratory (1960).
- Je63 J. M. F. Jeronimo, G. S. Mani, J. Olkowsky, A. Sadeghi, and C. F. Williamson, "Absolute Cross-Sections for Some (n,p), (n, $\alpha$ ), and (n,2n) Reactions," Nucl. Phys. 47, 157 (1963).
- Jo64 G. D. Joanou and C. A. Stevens, "Neutron Cross Sections for Aluminum," General Atomic Report GA-5884 (1964).
- Ju71 E. T. Journey, private communication (1971).
- Ka61 J. Kantele, "Activation Cross Sections for 14.5-MeV Neutrons for Bi, O<sub>16</sub>, Al<sup>27</sup>, and F<sup>19</sup>," Bull. Am. Phys. Soc. 6, 252 (1961).
- Ka62 J. Kantele and D. G. Gardner, "Some Activation Cross Sections for 14.7-MeV Neutrons," Nucl. Phys. 35, 353 (1962).
- Ka72 J. L. Kammerdiener, "Neutron Spectra Emitted by  $^{239}\text{Pu}$ ,  $^{238}\text{U}$ ,  $^{235}\text{U}$ , Pb, Nb, Ni, Al, and C Irradiated by 14-MeV Neutrons," Thesis, University of California at Davis (1972).
- Ke59 B. D. Kern, W. E. Thompson, and J. M. Ferguson, "Cross Sections for Some (n,p) and (n, $\alpha$ ) Reactions," Nucl. Phys. 10, 226 (1959).
- Kh58 M. M. Khaletskii, "Determination of Differential Elastic Scattering Cross Sections for 14.8-MeV Neutrons by (n, $\alpha$ ) Coincidences," Sov. Phys. -Dokl. 2, 152 (1958).
- Kh59 C. S. Khurana and H. S. Hans, "Measurements of (n,p), (n, $\alpha$ ), and (n,2n) Total Cross Sections at 14 MeV," Nucl. Phys. 13, 88 (1959).
- Ki70 W. E. Kinney and F. G. Perey, "Al Neutron Elastic- and Inelastic-Scattering Cross Sections from 4.19 to 8.56 MeV," Oak Ridge National Laboratory report ORNL-4516 (1970).
- Ko58 V. N. Kononov, Yu. Ya. Stavisskii, and V. A. Tolstikov, "Measurement of the Radiative Capture Cross Section of 25 keV Neutrons," At. Energiya 5, 564 (1958).
- Ko63 I. A. Korzh and N. T. Sklyar, "Angular Distribution of Neutrons of Energy 0.3 MeV Elastically Scattered by Atomic Nuclei," Ukr. Fiz. Zh. 8, 1389 (1963); I. A. Korzh, N. S. Kopytin, M. V. Pasechnik, N. M. Pravdivy, N. T. Sklyar, and I. A. Totsky, "Elastic Scattering of Neutrons with Energy 0.65 MeV by Atomic Nuclei," Ukr. Fiz. Zh. 8, 1323 (1963). These articles are in Ukrainian, not in Russian.
- Ko64 I. A. Korzh, N. S. Kopytin, M. V. Pasechnik, N. T. Sklyar, and I. A. Totsky, "Scattering of Neutrons with Energies 0.5 and 0.8 MeV by Light and Medium Nuclei," At. Energiya 16, 260 (1964); translated in Sov. J. At. En. 16, 312 (1965).
- La57 A. Langsdorf, Jr., R. O. Lang, and J. E. Monahan, "Angular Distributions of Scattered Neutrons," Phys. Rev. 107, 1077 (1957).
- La62 J. Langmann, private communication to Sigma Center, Brookhaven National Laboratory (1962).
- Le58 A. I. Leipunsky, O. D. Kazachkovsky, G. Y. Artyukhov, A. I. Baryshnikov, T. S. Belanova, V. I. Galkov, Yu. Ya. Stavisskii, E. A. Stumbur, and L. E. Sherman, "Measurements of Radiative Capture Cross Sections for Fast Neutrons," Proc. Intern. Conf. Peaceful Uses At. Energy, 2nd, Geneva, 1958 (United Nations, New York, 1959) Vol. 15, p. 50.
- L155 R. N. Little, Jr., B. P. Leonard, Jr., J. T. Prud'homme, and L. D. Vincent, "Liquid Scintillator Measurements of Angular Elastic Scattering of Neutrons from Carbon, Aluminum, and Sulfur," Phys. Rev. 98, 634 (1955).
- L166 H. Liskien and A. Paulsen, "Cross Sections for the  $\text{Cu}^{63}(n,\alpha)\text{Co}^{60}$ ,  $\text{Ni}^{60}(n,p)\text{Co}^{60}$ , and Some Other Threshold Reactions Using Neutrons from the  $\text{Be}^9(\alpha,n)\text{C}^{12}$  Reaction," Nukleonik 8, 315 (1966).
- Lo57 G. N. Lovchikova, "Measurement of the Angular Distribution of 0.9-MeV Neutrons Elastically Scattered on Bi, Pb, Sn, Fe, and Al," Sov. J. At. En. 2, 197 (1957).
- Lo60 G. N. Lovchikova, "Angular Distribution of Elastically Scattered Neutrons," Sov. Phys. -JETP 11, 1036 (1960).
- Ma57 M. H. MacGregor, W. P. Ball, and R. Booth, "Non-elastic Neutron Cross Sections at 14 MeV," Phys. Rev. 108, 726 (1957).
- Ma57a R. L. Macklin, N. H. Lazar, and W. S. Lyon, "Neutron Activation Cross Sections with Sb-Be Neutrons," Phys. Rev. 107, 504 (1957).
- Ma60 G. S. Mani, G. J. McCallum, and A. T. G. Ferguson, "Neutron Cross-Sections in Aluminium," Nucl. Phys. 19, 535 (1960).
- Ma63 R. L. Macklin, J. H. Gibbons, and T. Inada, "Average Radiative Capture Cross Sections for 30- and 65-keV Neutrons," Phys. Rev. 129, 2695 (1963).

- Ma65 S. C. Mathur, W. E. Tucker, R. W. Benjamin, and I. L. Morgan, "Angular Distributions of Gamma Rays Produced by Neutron Bombardment of Al, Mg, and Si," Nucl. Phys. 73, 561 (1965).
- Ma68 J. Martin, D. T. Stewart, and W. M. Currie, "Scattering of 6-MeV Neutrons from Light Nuclei," Nucl. Phys. A113, 564 (1968).
- Ma69 R. E. Maerker and F. J. Muckenthaler, "Gamma-Ray Spectra Arising from Thermal-Neutron Capture in Elements Found in Soils, Concretes, and Structural Materials," Oak Ridge National Laboratory report ORNL-4382 (1969).
- Me52 A. W. Merrison and E. R. Wiblin, "The Total Neutron Cross-Sections of Cobalt, Silver, Iodine, Aluminium, Nickel, and Gallium between 1 eV and 5 keV," Proc. Roy. Soc. (London) 215, 278 (1952).
- Me67 H. O. Menlove, K. L. Coop, H. A. Grench, and R. Sher, "Activation Cross Sections for the  $F19(n,2n)F18$ ,  $Na23(n,2n)Na22$ ,  $Mn55(n,2n)Mn54$ ,  $In115(n,2n)In114m$ ,  $Ho165(n,2n)Ho164m$ ,  $In115(n,n')In115m$ , and  $Al27(n,\alpha)Na24$  Reactions," Phys. Rev. 163, 1308 (1967).
- Mi66 B. Mitra and A. M. Ghose, "(n,p) Cross Sections of Some Low-Z Nuclei for 14.8-MeV Neutrons," Nucl. Phys. 83, 157 (1966).
- Mi67 B. Minetti and A. Pasquarelli, "Cross Sections of the (n,p) and (n, $\alpha$ ) Reactions Induced in Manganese by 14.7 MeV-Neutrons," Z. Physik 199, 275 (1967).
- Mi68 A. Mittler, K. C. Chung, M. T. McEllistrem, and J. D. Brandenberger, "Scattering of 8.0-MeV Neutrons from  $^{24}Mg$ ,  $^{27}Al$ ,  $^{28}Si$ ,  $^{31}P$ , and  $^{32}S$ ," Bull. Am. Phys. Soc. 13, 1420 (1968).
- Mu61 S. K. Mukherjee, A. K. Ganguly, and N. K. Majumder, "Activation Cross Sections with 14-MeV Neutrons," Proc. Phys. Soc. (London) 77, 508 (1961).
- Mu72 D. W. Muir, private communication (1972).
- Ne71 D. O. Nellis and P. S. Buchanan, "Neutron Scattering and Gamma-Ray Production Cross Sections for N, O, Al, Si, Ca, and Fe," private communication (1971).
- Ny69 K. Nyberg, B. Jönsson, and I. Bergqvist, "High-Resolution Measurements of Gamma Rays Produced by 15-MeV Neutrons," European-American Nuclear Data Committee report EANDC(OR)83-L (1969), p. 26.
- Or70 V. J. Orphan, N. C. Rasmussen, and T. L. Harper, "Line and Continuum Gamma-Ray Yields from Thermal-Neutron Capture in 75 Elements," Gulf General Atomic report GA-10248 (1970).
- Or71 V. J. Orphan and C. G. Hoot, "Gamma-Ray Production Cross Sections for Iron and Aluminum," Gulf Radiation Technology report GULF-RT-AL0743 (1971).
- Pa53 E. B. Paul and R. L. Clarke, "Cross-Section Measurements of Reactions Induced by Neutrons of 14.5 MeV Energy," Can. J. Phys. 31, 267 (1953).
- Pa55 M. V. Pasechnik, "Inelastic Scattering of Fast Neutrons by Atomic Nuclei," Proc. Intern. Conf. Peaceful Uses At. Energy, Geneva, 1955 (United Nations, New York, 1956), Vol. 2, p. 3.
- Pa65 A. Paulsen and H. Liskien, "Cross Sections for the Reactions  $^{55}Mn(n,2n)^{54}Mn$ ,  $^{59}Co(n,2n)^{58}Co$ ,  $^{24}Mg(n,p)^{24}Na$  and  $^{27}Al(n,\alpha)^{24}Na$  in the 12.6-19.6 MeV Energy Region," J. Nucl. Energy, Parts A/B 19, 907 (1965).
- Pa70 D. Partington, D. Crumpton, and S. E. Hunt, "Determination of the Energy Dependence of the  $^{63}Cu(n,2n)^{62}Cu$  and  $^{27}Al(n,p)^{27}Mg$  Cross-Sections, and their Application to the Measurement of 14-MeV Neutron Fluxes," Analyst 95, 257 (1970).
- Pe57 J. L. Perkin, L. P. O'Connor, and R. F. Coleman, "Radiative Capture Cross Sections for 14.5-MeV Neutrons," Proc. Phys. Soc. (London) 72, 505 (1958).
- Pe64 J. L. Perkin, "Gamma Ray Spectra from Fast Neutron Interactions," Nucl. Phys. 60, 561 (1964).
- Pe67 G. Petö, Z. Miligy, and I. Hunyadi, "Radiative-Capture Cross Sections for 3-MeV Neutrons," J. Nucl. En. 21, 797 (1967).
- Ph52 D. D. Phillips, R. W. Davis, and E. R. Graves, "Inelastic Collision Cross Sections for 14-MeV Neutrons," Phys. Rev. 88, 600 (1952).
- Po56 Kh. R. Poze and N. P. Glazkov, "Inelastic Scattering of 0.3, 0.77, and 1.0 MeV Photoneutrons," Sov. Phys. -JETP 3, 745 (1956).
- Po59 A. Poularikas and R. W. Fink, "Absolute Activation Cross Sections for Reactions of Bismuth, Copper, Titanium, and Aluminum with 14.8-MeV Neutrons," Phys. Rev. 115, 989 (1959).
- Po61 H. Pollehn and H. Neuert, "Bestimmung von Wirkungsquerschnitten einiger Kernreaktionen durch 14 MeV-Neutronen nach einer Aktivierungsmethode," Z. Naturforsch. 16A, 227 (1961).
- Po61a V. I. Popov, "Angle Distribution of 3.1-MeV Neutrons Elastically Scattered on Al, Si, K, Ca, and Th," Soviet Progress in Neutron Physics (Gosatomizdat, Moscow, 1961; translated by Consultants Bureau Enterprises, New York, 1963), p. 224.
- Pr60 J. T. Prud'homme, I. L. Morgan, J. H. McCrary, J. B. Ashe, and O. M. Hudson, Jr., "A Study of Neutrons and Gamma Rays from Neutron Induced Reactions in Several Elements," Air Force Special Weapons Center report AFSWC-TR-60-30 (1960).
- Ra65 L. A. Rayburn and E. O. Wollan, "Total Neutron Cross Sections at 1.44 eV," Nucl. Phys. 61, 381 (1965).
- Ra68 N. Ranakumar, E. Kondaiah, and R. W. Fink, "Neutron Activation Cross Sections at 14.4 MeV for Si and Zn Isotopes," Nucl. Phys. A122, 679 (1968).
- Ro68 H. Röpke and S. T. Lam, "A Study of the 4.509-MeV State in  $^{27}Al$  by the  $^{26}Mg(p,\gamma)$  Reaction," Can. J. Phys. 46, 1649 (1968).

- Ro69 H. Röpke and N. Anyas-Weiss, "The  $^{23}\text{Na}(\alpha, \gamma)^{27}\text{Al}$  Reaction. A Survey of the Reaction and Some Properties of the  $^{27}\text{Al}$  Nucleus," *Can. J. Phys.* 47, 1545 (1969).
- Sa59 C. St. Pierre, M. K. Machwe, and P. Lorrain, "Elastic Scattering of 14-MeV Neutrons by Al, S, Ti, and Co," *Phys. Rev.* 115, 999 (1959).
- Sa61 M. Sakisaka, B. Saeki, M. Tomita, and F. Fukuzawa, "Sample-Sandwiched Plastic Scintillators for Activation Measurements by Use of Fast Neutrons," *J. Phys. Soc. Japan* 16, 1869 (1961).
- Sa71 G. N. Salaita, "Absolute Neutron Cross Sections for the Production of the  $^{24}\text{Na}$  Isomer from Magnesium and Aluminum," *Nucl. Phys.* A170, 193 (1971).
- Sc53 V. E. Scherrer, R. B. Theus, and W. R. Faust, "Gamma-Rays from Interaction of 14-MeV Neutrons with Various Materials," *Phys. Rev.* 91, 1476 (1953).
- Sc61 H. W. Schmitt and J. Halperin, " $\text{Al}^{27}(\text{n}, \alpha)\text{Na}^{24}$  Cross Section as a Function of Neutron Energy," *Phys. Rev.* 121, 827 (1961).
- Sc66 R. M. Schectman and J. D. Anderson, "Inelastic Scattering of 14-MeV Neutrons," *Nucl. Phys.* 77, 241 (1966).
- Sc70 R. B. Schwartz, private communication (1970).
- Se47 L. Seren, H. N. Friedlander, and S. H. Turkel, "Thermal Neutron Activation Cross Sections," *Phys. Rev.* 72, 888 (1947).
- Sh62 R. Sher and B. A. Magurno, private communication to R. J. Howerton, Lawrence Livermore Laboratory (1962).
- St57 V. I. Strizhak, "Inelastic Interaction of 14-MeV Neutrons with Nuclei," *At. Energiya* 2, 68 (1957).
- St62 T. P. Stuart, J. D. Anderson, and C. Wong, "Elastic Scattering of 24-MeV Neutrons by Al, Fe, Sn, Bi," *Phys. Rev.* 125, 276 (1962).
- St62a P. Strohal, N. Cindro, and B. Eman, "Reaction Mechanism and Shell Effects from the Interaction of 14.6-MeV Neutrons with Nuclei," *Nucl. Phys.* 30, 49 (1962).
- St65 P. H. Stelson, R. L. Robinson, H. J. Kim, J. Rapaport, and G. R. Satchler, "Excitation of Collective States by the Inelastic Scattering of 14 MeV Neutrons," *Nucl. Phys.* 68, 97 (1965).
- St65a J. E. Strain and W. J. Ross, "14-MeV Neutron Reactions," Oak Ridge National Laboratory report ORNL-3672 (1965).
- Ta55 H. L. Taylor, O. Lönsjö, and T. W. Bonner, "Non-elastic Scattering Cross Sections for Fast Neutrons," *Phys. Rev.* 100, 174 (1955).
- Ta69 S. Tanaka, K. Tsukada, Y. Tomita, and M. Maruyama, "Differential Cross Sections of Aluminum and Silicon for the Elastic and Inelastic Scattering of Neutrons," private communication to W. E. Kinney from Tanaka et al. (1969); "Fast Neutron Scattering from Al, Si, S, and Zn," *Nuclear Data for Reactors* (International Atomic Energy Agency, Vienna, 1970), p 317.
- Te60 H. A. Tewes, A. A. Caretto, A. E. Miller, and D. R. Nethaway, "Excitation Functions of Neutron Induced Reactions," University of California Radiation Laboratory report UCRL-6028-T (1960).
- Th63 D. B. Thomson, "Nuclear Level Densities and Reaction Mechanisms from Inelastic Neutron Scattering," *Phys. Rev.* 129, 1649 (1963).
- Th65 W. E. Thompson and F. C. Engesser, "Gamma Rays from Interactions of 14.7-MeV Neutrons with Magnesium, Aluminum, Calcium, Titanium, and Iron," United States Naval Radiological Defense Laboratory report USNRDL-TR-861 (1965); F. C. Engesser and W. G. Thompson, "Gamma Rays Resulting from Interactions of 14.7-MeV Neutrons with Various Elements," *J. Nucl. Eng.* 21, 487 (1967).
- Ti68 P. N. Tiwari and E. Kondaiah, "Activation Cross Sections of Calcium, Potassium, and Aluminum for 14.2-MeV Neutrons," *Phys. Rev.* 167, 1091 (1968).
- To62 J. H. Towle and W. B. Gilboy, "Spin Assignments in  $\text{Al}^{27}$  from Neutron Scattering Studies," *Nucl. Phys.* 39, 300 (1962).
- To67 J. H. Towle and R. O. Owens, "Absolute Level Densities from Neutron Inelastic Scattering," *Nucl. Phys.* A100, 257 (1967).
- Tr61 E. S. Troubetzkoy, "Statistical Theory of Gamma-Ray Spectra Following Nuclear Reactions," *Phys. Rev.* 122, 212 (1961).
- Ts61 K. Tsukada, S. Tanaka, M. Maruyama, and Y. Tomita, "Angular Distributions of Fast Neutrons Scattered by Al, Si, P, S, and Zn," *Proc. Seminar Phys. Fast and Intermediate Reactors, Vienna, 1961* (International Atomic Energy Agency, Vienna, 1962), p. 75.
- Va67 C. van der Leun, D. M. Sheppard, and P. M. Endt, "The Reaction  $^{26}\text{Mg}(p, \gamma)^{27}\text{Al}$ ," *Nucl. Phys.* A100, 316 (1967).
- Ve58 J. F. Vervier, "Section Efficace de Capture Radiative pour des Neutrons d'une Source Sb-Be," *Nucl. Phys.* 9, 569 (1958/59).
- Wa55 M. Walt and J. R. Beyster, "Interaction of 4.1-MeV Neutrons with Nuclei," *Phys. Rev.* 98, 677 (1955).
- Wi49 G. C. Wick, "A Theorem on Cross Sections," *Phys. Rev.* 75, 1459 (1949).
- Wi63 D. Winterhalter, "Angular Distributions of Fast Neutrons Scattered on Aluminium," *Nucl. Phys.* 43, 339 (1963).

- Ya57 S. Yasumi, "Nuclear Reactions Induced by the 14-MeV Neutrons," J. Phys. Soc. Japan 12, 443 (1957).
- Yu58 K. Yuasa, "Differential Elastic Scattering of 14-MeV Neutrons in Aluminum, Lead, and Bismuth for Large Angles," J. Phys. Soc. Japan 13, 1248 (1958).